

BNWL-1875
UC-78

11A

PREDICTION OF FISSION GAS
RELEASE FROM UO_2 FUEL



Battelle

Pacific Northwest Laboratories
Richland, Washington 99352

NOVEMBER 1974

Prepared for the U.S. Atomic Energy
Commission under Contract AT(45-1):1830

BNWL-1875

NOTICE

This report was prepared as an account of work sponsored by the United States Government. Neither the United States nor the United States Atomic Energy Commission, nor any of their employees, nor any of their contractors, subcontractors, or their employees, makes any warranty, express or implied, or assumes any legal liability or responsibility for the accuracy, completeness or usefulness of any information, apparatus, product or process disclosed, or represents that its use would not infringe privately owned rights.

PACIFIC NORTHWEST LABORATORY
operated by
BATTELLE
for the
U.S. ATOMIC ENERGY COMMISSION
Under Contract AT(45-1)-1830

Printed in the United States of America
Available from
National Technical Information Service
U.S. Department of Commerce
5285 Port Royal Road
Springfield, Virginia 22151
Price: Printed Copy \$7.60; Microfiche \$2.25

ERRATA

BNWL-1875

PREDICTION OF FISSION GAS RELEASE FROM UO₂ FUEL

by

C. E. Beyer

C. R. Hann

On page 22 change the following equation

$$F = 0.050 X_1 + 0.141 X_2 + 0.807 X_3 + 1.68 (0.002112 + 0.0052 X_2^2 - 0.00269 X_2 X_3 + 0.00217 X_3^2)$$

to read

$$F = 0.050 X_1 + 0.141 X_2 + 0.807 X_3 + 1.68 \left(0.002112 + 0.0052 X_2^2 - 0.00269 X_2 X_3 + 0.00217 X_3^2 \right)^{1/2}$$

On page 26 the second line of the text reads "...shows that there is ~50% chance that D = 0 and K = 0 and thus indicates...", change ~50% to ~30%.

3 3679 00062 5238

BNWL-1875
UC-78

PREDICTION OF FISSION GAS
RELEASE FROM UO_2 FUEL

by
C. E. Beyer
and
C. R. Hann

November 1974

BATTELLE
PACIFIC NORTHWEST LABORATORIES
RICHLAND, WASHINGTON 99352

TABLE OF CONTENTS

1.0	INTRODUCTION	1
2.0	SUMMARY AND CONCLUSIONS	3
3.0	HIGH TEMPERATURE GAS RELEASE MODEL	4
3.1	DATA SELECTION	4
3.2	DATA REDUCTION	10
3.3	MODELS REVIEWED FOR HIGH TEMPERATURE GAS RELEASE	13
3.3.1	Volume Averaged Fuel Temperature	14
3.3.2	Theoretical Model	15
3.3.3	Local Temperature Distribution	16
3.3.4	Effective Diffusion Coefficient Model	16
3.4	SELECTION OF HIGH TEMPERATURE GAS RELEASE MODEL	18
3.4.1	Columnar Grain Growth Region	18
3.4.2	Equiaxed Grain Growth Region	18
3.4.3	Region of No Microstructural Change	19
3.4.4	Description of Model	19
3.5	CORRELATING THE MODEL TO THE DATA	20
3.6	EFFECTS OF DENSITY AND BURNUP	25
4.0	LOW TEMPERATURE GAS RELEASE MODEL	27
4.1	DEVELOPMENT OF THE MODEL	27
5.0	LIMITATIONS OF THE GAS RELEASE MODELS	31
	ACKNOWLEDGEMENTS	32
	REFERENCES	33
	APPENDIX A	A-1
	APPENDIX B	B-1

PREDICTION OF FISSION GAS RELEASE FROM UO_2 FUEL

C. E. Beyer and C. R. Hann

1.0 INTRODUCTION

High temperature ($>1200^\circ\text{C}$) gas release from UO_2 fuel is an important consideration in steady state reactor safety calculations because of its effect on the fuel-to-cladding gap conductance (and thus fuel temperatures) and fuel rod internal gas pressures. Conservative and best-estimate correlations for gas release are needed to initialize gap conductance and internal pressure in the rod before accident calculations can be performed. Several methods for calculating the high temperature fission gas release have been proposed¹⁻⁷ but the results vary widely. However, most investigators agree that high temperature gas release is a nonlinear phenomenon which is dependent upon local conditions in the fuel, with fuel temperature being the primary controlling parameter. The large uncertainties that are inherent in estimating fuel temperatures often preclude a reliable correlation for gas release. These uncertainties in determining fuel temperatures, plus the inherent differences in the models themselves, account for the lack of agreement between previously proposed models.

Low temperature ($<1200^\circ\text{C}$) gas release from fuel with burnups of less than 20,000 MWD/MTM is typically in the range of 2% or lower. The release from low temperature fuel is not as significant as the high temperature release because the gap conductance and internal rod pressures change very little when gas release is on the order of 2%. A low temperature release model will be used to extend gas release predictions below temperatures of 1200°C .

The objectives of the work reported here were:

- to evaluate the open literature data and select those data that were well characterized with regard to high temperature gas release and fuel temperatures,

- to reduce the selected data to a useful form by employing a consistent and documented method,
- to select a model (or models) which best describes these data and is consistent with known theory and phenomenology of gas release from light water reactor (LWR) UO_2 fuel, and
- to correlate the gas release model (or models) against these data.

2.0 SUMMARY AND CONCLUSIONS

High and low temperature gas release models were developed to provide an improved method for predicting gas release from UO₂ fuel because of the important role of fission gas release in LWR safety calculations. The high temperature release model was fit to a consistent and well characterized set of 45 data points using a multiple linear regression code. The low temperature release model is a modification of one developed by Bellamy and Rich⁸ and is compatible with the high temperature model (i.e., extends gas release predictions to temperatures below 1200°C where the high temperature model is not applicable).

The conclusions reached as a result of this study are:

1. The high temperature gas release model fits the data well with a correlation coefficient of 0.980 and a standard deviation of 4.7 in percent release.
2. In the operating range of current design light water reactors, previously proposed high temperature release models are more conservative (i.e., predict larger gas release fractions) than the model developed here.
3. Power histories, large axial power gradients, and fuel temperature estimates seem to be the major factors which cause the large variance among gas release data. A definite reduction in the variance results if the above parameters are controlled.
4. Burnup and density have no detectable influence on high temperature gas release over the range 400 to 18,000 MWD/MTM and 91.3 to 98.0% theoretical density.
5. Experimental data indicate that low temperature gas release increases with increasing burnup for burnups greater than 20,000 MWD/MTM.

3.0 HIGH TEMPERATURE GAS RELEASE MODEL

3.1 DATA SELECTION

From the open literature 74 sources¹⁻⁷⁴ for high temperature gas release information were examined. Some sources did not supply new data but did propose and discuss various models for gas release, while others provided data on gas release that were not applicable to light water reactor UO₂ fuels. Table 1 is a list of the sources and the data used in correlating the high temperature model. Before discussing these data in detail we will provide some background on 1) the methods used to measure gas release, 2) the methods which provide data applicable to current commercial reactor fuels, and 3) the general rationale we have used to select data for the correlation.

Data from out-of-reactor tests were not used because out-of-reactor gas release data typically do not agree well with in-reactor release data. Out-of-reactor tests usually consist of postirradiation annealing studies wherein irradiated fuel is heated in the laboratory while simultaneously monitoring the release of gas. Results from these tests do not agree with in-reactor release because the fuel is subjected to different environments. Laboratory annealing tests involve isothermal heating of fuel, while in-reactor fuel is subjected to severe temperature gradients on the order of 4000°C/cm. Current theories^{17,18} indicate that temperature gradients have a strong influence on gas release. Laboratory tests also do not subject the fuel to the continuing perturbations created by the fissioning process. These perturbations are thought to both impede and enhance gas movement. The gas is impeded by the creation of structural defects within the fuel matrix which can trap the gas either in the form of an atom or bubble. Fission spiking can enhance gas release by 1) enabling the gas atom to break away from these traps, or 2) if the gas is in bubble form it can promote resolution of the trapped bubble.

In-reactor tests for measuring gas release can be separated into two categories. The first employs a sweep gas technique while the second

TABLE 1. High Temperature Gas Release Data

REFERENCE	SPECIMEN NUMBER	ENRICHMENT (WT % ²³⁵ U)	PELLET DIAMETER OD/ID (IN.)	FUEL LENGTH (IN.)	HEAT RATING (KW/FT)	BURNUP (MWD/MTM)	GRAIN GROWTH		PELLET DENSITY (%TD)	GAS RELEASE (PERCENT)	
							EQUIAXED (R/R ₀)	COLUMNAR (R/R ₀)			
CYRANO-(9, 10)* EXP.	CYRANO-11	4.0	0.433/0.0472	3.94	13.9	940	1990/2069 ^o C**	-	96.4	15.0	
	CYRANO-111	DID NOT USE	BECAUSE POWER HISTORY VARIED	~20%	-	-	-	-	-	-	
HPR-129 (11)*	CYRANO-VIII	4.0	0.512/0.0472	3.94	11.5	1282	1890/1969 ^o C**	-	94.8	13.0	
	116-1	DID NOT USE	BECAUSE THERMOCOUPLE FAILURE WAS SUSPECTED EARLY IN LIFE	-	-	-	-	-	-	-	
BELGONUCLEAIRE (12) AND CEA	116-5	6.0	0.541/0.126	19.0	22.8	4223	2070/2374 ^o C**	-	91.3	27.5	
	117-1	6.0	0.5451/0.126	19.0	21.0	7148	2060/2329 ^o C**	-	96.9	25.4	
	117-5	DID NOT USE	BECAUSE OF THERMOCOUPLE FAILURE EARLY IN LIFE	-	-	-	-	-	-	-	
	117-6	DID NOT USE	BECAUSE OF LARGE AXIAL FLUX GRADIENT ACROSS THE PIN	-	-	-	-	-	-	-	
	EPL-3	DID NOT USE	BECAUSE POWER HISTORY VARIED	~16%	-	-	-	-	-	-	
AECL-2662 (13)	EPL-4	2.4	0.2921	-	39.37	12.3	11,100	0.5256	-	93.9	9.9
	EPL-5	2.4	0.2921	-	39.37	13.5	3990	0.4582	-	93.9	4.4
	EPL-6	2.4	0.2921	-	39.37	15.1	14,400	0.6873	.5445	93.9	21.3
	EPL-7	DID NOT USE	BECAUSE POWER HISTORY VARIED	~20%	-	-	-	-	-	-	
	EPL-8	DID NOT USE	BECAUSE POWER HISTORY VARIED	~20%	-	-	-	-	-	-	
	EPL-9	2.4	0.2921	-	39.37	14.9	18,300	0.6119	.4582	93.9	23.2
	EPL-10	2.4	0.2921	-	39.37	14.9	9940	0.6280	.4906	93.9	18.3
	EPL-11	DID NOT USE	BECAUSE POWER HISTORY VARIED	~20%	-	-	-	-	-	-	
	EPL-12	2.4	0.2921	-	39.37	13.3	8440	0.6388	.4232	93.9	17.8
	AECL-2230 (14) (TEST X-501)	LFL	2.40	0.7638	9.57	18.0	2230	0.375	-	98.0	5.7
		LFF	2.40	0.7638	9.57	17.8	2230	0.582	-	95.7	17.3
LFB		2.40	0.7638	9.57	17.3	2230	0.642	0.497	93.4	23.4	
LFS		2.40	0.7638	9.57	24.5	3120	0.697	0.631	98.0	37.9	
LFW		2.40	0.7638	9.57	25.0	3290	0.640	0.575	98.0	24.8	
LFT		2.40	0.7638	9.57	24.1	3290	0.735	0.659	93.4	49.6	
LFX		2.40	0.7638	9.57	24.9	3290	0.715	0.646	95.7	36.8	
LFK		2.40	0.7638	9.57	24.3	3120	0.712	0.633	-	-	
LFM		2.40	0.7638	9.57	22.7	3030	0.609	0.536	98.0	15.5	
LFH		2.40	0.7638	9.57	22.1	3030	0.702	0.602	95.7	31.1	
LFD		2.40	0.7638	9.57	22.1	3030	0.743	0.679	93.4	45.8	
AECL-1676 (15) (TEST X-211)		C BN	4.5	0.6429	6.02	17.1	2650	0.51	0.31	97.9	12.3
		C BO	4.5	0.6425	6.02	17.3	2670	0.52	0.37	97.8	14.9
	C BP	4.5	0.6425	6.02	16.8	2610	0.50	0.33	97.2	14.1	
	C BR	4.5	0.642	6.02	17.4	2710	0.56	0.44	97.1	15.7	
	C BT	4.5	0.6425	6.02	16.6	2620	0.52	0.43	96.2	15.3	
	C BV	4.5	0.6425	6.02	17.5	2760	0.54	0.45	95.9	16.5	
	C BY	4.5	0.6425	6.02	16.55	2630	0.55	0.47	95.0	16.8	
	C BX	4.5	0.6425	6.02	17.1	2720	0.57	0.51	95.2	18.8	
	CEA-R-3358 (16)	DFE	4.34	0.748	6.26	35.8	794	-	0.74	96.6	40.1
DFH		4.34	0.748	6.26	29.5	648	-	0.67	96.6	32.6	
DFD		4.34	0.748	6.26	29.05	658	-	0.70	96.6	33.0	
DFJ		DID NOT USE	BECAUSE POWER HISTORY VARIED	~17%	-	-	-	-	-	-	
DFB		4.34	0.748	6.26	24.0	528	-	0.597	96.6	17.9	
DFA		4.34	0.748	6.26	17.7	386	-	0.460	96.6	4.95	
4110-AE1		2.98	0.5094	4.84	18.1	6416	0.6934	-	96.0	21.6	
-AE2	2.98	0.5094	4.84	17.6	6243	0.6549	-	96.0	22.1		
-BE1	2.98	0.5094	4.84	15.1	5222	0.5639	-	96.0	13.9		
-BE2	2.98	0.5094	4.84	17.8	6566	0.6009	-	96.0	15.9		
4111-AE1	DID NOT USE	BECAUSE POWER HISTORY VARIED	~20%	-	-	-	-	-	-		
-AE2	DID NOT USE	BECAUSE POWER HISTORY VARIED	~20%	-	-	-	-	-	-		
-BE1	DID NOT USE	BECAUSE POWER HISTORY VARIED	~20%	-	-	-	-	-	-		
-BE2	DID NOT USE	BECAUSE POWER HISTORY VARIED	~20%	-	-	-	-	-	-		
4112-AE1	2.98	0.5111	4.84	19.5	3453	0.6225	0.431	95.0	12.6		
-AE2	2.98	0.5110	4.84	17.7	3230	0.6133	0.421	95.0	11.2		
-BE1	2.98	0.5111	4.84	15.4	2796	0.4330	-	95.0	7.9		
-BE2	2.98	0.5110	4.84	16.6	3015	0.5794	0.279	95.0	12.6		
4113-AE1	2.98	0.5138	4.84	17.1	3110	0.7627	0.644	95.0	26.7		
-AE2	2.98	0.5138	4.84	15.6	2836	0.7442	0.564	95.0	28.0		
-BE1	2.98	0.5138	4.84	16.0	2843	0.5794	0.411	95.0	17.0		
-BE2	2.98	0.5138	4.84	15.9	2895	0.7190	0.548	95.0	21.0		

* FUEL TEMPERATURES DETERMINED WITH THERMOCOUPLES

** TEMPERATURE MEASUREMENT BY A THERMOCOUPLE AT FUEL CENTERLINE/CORRECTED CENTERLINE TEMPERATURES FOR THAT PORTION OF THE FUEL WITHOUT AN ANNULAR HOLE AND THERMOCOUPLE

utilizes sealed capsule irradiations. Sweep gas experiments are based on continually collecting and monitoring the gas given off during irradiation. The amount of gas released in sealed capsule experiments is determined by destructive examination after the fuel has been irradiated for a specified period of time. The data generated by the sweep gas technique are generally obtained from fuel operating at low heat ratings and thus temperature gradients within the fuel are small. Consequently, sweep gas experiments may yield atypical results because temperature gradients are believed to have a substantial effect on gas release in commercial fuel. A comparison of sealed capsule data at heat ratings >5 kW/ft with sweep gas data^{19,20} obtained at lower heat ratings but with similar fuel temperatures (1700-2000°C) shows significant differences (e.g., sweep gas release data are often more than an order of magnitude lower). Consequently, sweep gas tests using low heat ratings were not considered for our correlation. Data from the CYRANO experiments^{9,10} which used the sweep gas technique were used in our correlation; however, these experiments operated with heat ratings large enough (10-15 kW/ft) to have a substantial thermal gradient ($>2500^{\circ}\text{C}/\text{cm}$) and thus provide relevant data. The remaining data in Table 1 come from sealed capsule experiments wherein gas release was determined by destructive postirradiation examination.

To reduce the amount of variability in the gas release data, we have identified four factors (listed in Table 2) that might enhance this variability and used them as data selection criteria. These are:

1. Stoichiometry
2. Variable power operation
3. Variable axial power generation
4. Imprecise fuel temperature determinations

It has been shown that hyper-stoichiometric UO_2 has significantly higher fission gas release than stoichiometric UO_2 .²¹ This is not unexpected since Xe and Kr have higher diffusion rates in hyper-stoichiometric UO_2 .^{22,23}

Soulhier and Notley²⁴ have shown that variable power histories can have a significant effect on gas release; this also may be expected since variation in power is reflected by a temperature variation.

TABLE 2. Rationale for Establishing
Criteria for Data Selection

Factors That Enhance the Variability of Gas Release	Criteria for the Selection of Data
1. Stoichiometry	1. Only stoichiometric UO ₂ (O/M 2.00 ±0.005) data were selected
2. Variable power operation	2. Only those data with a relatively constant power operating history were considered. The maximum power (P _{max}) over the life of a fuel pin cannot be more than 15% greater than the time averaged power (P _{time avg}) (i.e., $\frac{P_{max}}{P_{time\ avg}} \leq 1.15$)
3. Variable axial power generation	3. Only those experiments with short fuel columns and relatively flat axial power distributions were selected $\left(\frac{Peak\ Power}{Avg\ Power}\right) \leq 1.15$
4. Imprecise fuel temperature determinations	4. Only those experiments where fuel temperatures were either measured at a particular point in the fuel or could be inferred from a micro-structural change were considered

A large variation in the axial power profile will result in a large axial variation in fuel temperature, changing the gas release fractions along the length of the fuel. Correlating the total release of such a fuel rod with the average temperature of the fuel rod can lead to errors because gas release along the length of the rod is not linearly dependent on temperature.

Finally, the uncertainties in estimating fuel temperatures contribute significantly to the variability of gas release data. Past methods have resulted in significant uncertainties because fuel temperatures were seldom

measured by thermocouples or inferred from temperature indicators such as grain growth radii. Temperatures were usually estimated through more indirect methods, such as making some assumption about the value for gap conductance. Furthermore, different values for thermal conductivity, grain growth temperatures, and flux depressions were used by previous investigators.

Assuming a gap conductance can lead to substantial errors in fuel temperatures because gap conductance has been shown to be a very difficult parameter to estimate without previous knowledge of fuel temperatures. For example, a fuel rod with a heat rating of 11 kW/ft with the hot fuel-to-clad gap open can easily have a gas conductance of 600 Btu/hr-ft²-°F with a fuel centerline temperature of 1615°C. However, if the hot fuel-to-clad gap were closed in this same fuel rod a gap conductance of ≈5000 Btu/hr-ft²-°F would not be unreasonable which would result in a centerline temperature of 1180°C.

Our evaluation of the gas release data indicates that the last three factors (variable power operation, variable axial powers, and imprecise temperature estimates) contributed the most to the large amount of variance among gas release data. Nonstoichiometric fuel was a problem in early irradiation tests;²¹ however, stoichiometry was well controlled in later tests. The criteria used for the data selection is an attempt to reduce the variability of these four factors and thus the variability of the data. Of the 74 literature sources evaluated, 18 were selected which supplied gas release data applicable to LWR UO₂ fuel. Further evaluation of these 18 sources to determine whether they met the requirements listed in Table 2 resulted in rejection of experimental data from 11 of them. These data are listed in Table 3 along with the specific reasons for their rejection. The rejection of these particular experiments does not mean that they were not well characterized or executed, because the main objective of most of these experiments was not to evaluate gas release but other fuel performance parameters.

Not all data from the experiments selected (listed in Table 1) were used because some of the data did not meet the criteria listed in Table 2.

TABLE 3. References Rejected Which Contained Data Applicable to LWRs

Reference	Reason for Rejection
1. M.G. Balfour, "CVTR Fission Gas Release," WCAP-3850-5.	1. No data given from which temperatures could be determined. Temperature gradients in the axial direction were too large (axial $\frac{\text{Peak}}{\text{avg.}}$ power > 1.15).
2. W.A. Bezella, "Analysis of the Fission Gases Released Within Spent Yankee Fuel Rods," WCAP-6087.	2. No temperature data given. Power history varied too much ($\frac{P_{\text{max}}}{P_{\text{time avg.}}} > 1.15$)
3. F.A. Brandt, et al., "Irrad. Results, N.S. Savannah Core II Prototype Fuel Assemb. (Assemb. SAV-II-2 & SAV-II-3)," GEAP-3559.	3. Power history varied too much ($\frac{P_{\text{max}}}{P_{\text{time avg.}}} > 1.15$) Axial $\frac{\text{Peak}}{\text{avg.}}$ power > 1.15.
4. J.P. Hoffman, et al., "The Release of Fission Gases from Uranium Dioxide Pellet Fuel at High Temperatures," GEAP-4596.	4. No temperature data given. Axial $\frac{\text{Peak}}{\text{avg.}}$ power > 1.15.
5. C. Lepsky, et al., "Experimental Investigation of In-Reactor Molten Fuel Performance," Nucl. Tech. Vol. 16.	5. Axial $\frac{\text{Peak}}{\text{avg.}}$ power > 1.15. Vipac fuel, 85% T.D.
6. R.D. MacDonald, et al., "10,000 MWD/Tonne from UO ₂ Clad in This Zircaloy," Trans. Am. Nucl. Soc., 7, 449-450.	6. No temperature data given. Power history varied too much ($\frac{P_{\text{max}}}{P_{\text{time avg.}}} > 1.15$)
7. R.D. Page, "Engineering and Performance of Canada's UO ₂ Fuel Assemblies for Heavy Water Power Reactors," IAEA Symp. on Heavy Water Reactors, Vienna (1967).	7. No temperature data given. O/M ratios > 2.005.
8. R. Soulhier, et.al., "Effect of Power Changes on Fission Product Gas Release from UO ₂ Fuel," Nucl. Appl. Vol. 5.	8. No temperature data given.
9. C.N. Spalaris, et.al., "Residual and Fission Gas Release from UO ₂ ," GEAP-4314.	9. No temperature data given. Axial $\frac{\text{Peak}}{\text{avg.}}$ power > 1.15.
10. W.J. Zielenbach, et.al., "Irradiation Behavior of Oxide Fuels at High Temperatures," BMI-1925.	10. No temperature data given.
11. D.L. Zimmerman, "Irradiation and Postirradiation Examination of N.S. Savannah Test Fuel Element S1-A," GEAP-3342.	11. No temperature data given. Power history varied too much ($\frac{P_{\text{max}}}{P_{\text{time avg.}}} > 1.15$). Axial $\frac{\text{Peak}}{\text{avg.}}$ power > 1.15.

while others experienced thermocouple failures early in life. The specific reasons for the rejections of these data are included in Table 1. This table also shows the relatively small number of experiments that have concurrently used thermocouples to measure fuel temperatures while measuring the amount of gas release.

3.2 DATA REDUCTION

The data from the selected experiments have been reduced to obtain a radial fuel temperature profile for each data point using consistent values for UO_2 thermal conductivity and grain growth temperatures. The reduced data in terms of fuel centerline and surface temperatures are supplied in a table in Appendix B. One dimensional heat transfer with one axial node was used in calculating fuel temperatures (which is consistent with the relatively flat axial power distribution and the short fuel lengths).

Calculating the radial temperature profile of a cylindrical fuel column requires the following information:

- operating power of the fuel rod,
- thermal conductivity of the fuel,
- flux depression across the fuel radius, and
- fuel temperature at a known position.

A computer code, MAIN, was used to calculate radial temperature profiles. A listing and description of the code is provided in Appendix A.

The time-averaged power output of the fuel was used in these calculations and we selected only data in which the power histories varied less than 15% from the time-averaged power. The thermal conductivity equation derived by Lyons, et al.,^{76,77} for 95% TD UO_2 was used, along with the Maxwell-Euken^{78,79} relationship to account for effects of porosity on UO_2 thermal conductivity. Flux depressions for fuel with enrichments less than 4 wt% U-235 were estimated by use of a flux depression subroutine from the GAPON-THERMAL-1 code.⁸⁰ For enrichments greater than 4 wt% U-235, we have used a method proposed by Robertson.⁸¹ Good agreement is obtained in comparing these two methods for calculating flux depressions

with a more sophisticated neutronics code, THERMOS.⁸² One of the criteria set down in Table 2 for the selection of gas release data was that fuel temperatures must be obtained by the use of thermocouples or from the observation of microstructural changes in the fuel such as equiaxed and columnar grain growth. The temperatures associated with equiaxed and columnar grain growth boundaries are somewhat uncertain with the following temperature ranges having been proposed in the past:^{10,16,83-85}

- 1300 - 1500°C for equiaxed grain growth
- 1600 - 1800°C for columnar grain growth

Grain growth has been reported for higher temperatures than those listed above; however, the time-temperature relationship for grain growth at short times can be used to explain the differences. Hausner^{86,87} has reported out-of-reactor equiaxed grain growth results for pellets fabricated by 5 different procedures. These results were obtained from tests performed at temperatures between 1900-2300°C and times of 100 hours or less. Due to the different grain growth characteristics of pellets from each fabrication method, Hausner used the data to develop a time-temperature relationship for each of the 5 groups. An extrapolation of these relationships to lower temperatures and longer times indicates that grain growth is possible at 1400-1500°C for times between 10 and 500 hours.

Ainscough, et al.⁸⁸ have indicated that equiaxed grain growth asymptotes to a limiting grain size for a specific temperature at relatively long times (200-700 hours) and that while out-of-reactor grain growth results agree qualitatively with in-reactor results, the latter will have smaller limiting grain sizes due to the retarding effect of fission products with increasing burnup. Ainscough presents in-reactor data that show for temperatures of 1300°C, 1400°C and 1500°C the limiting grain sizes are 7.8 μ , 11.5 μ and 16.5 μ respectively. Thus an initial grain size between 6-8 μ would require a temperature of 1350-1400°C for the onset of grain growth to be observed. Similarly, an initial grain size of 12-14 μ would require a temperature of 1450-1500°C. It should be pointed out, however, that the assumptions used

by Ainscough to obtain in-reactor fuel temperatures were not available, making it impossible to estimate the uncertainties in these temperatures.

The initial grain sizes for 24 of the 45 selected data points were obtained. They vary between 4 to 37μ with a mean of 13μ . If a dependency existed between initial grain size and equiaxed grain growth temperature we would expect to over-predict temperatures and gas release for a small grained fuel and under-predict temperatures and gas release for a large grained fuel by choosing a 1400°C temperature for equiaxed grain growth (as we have done below). However, we have not observed such an effect over the range of the data. This does not mean that no such dependency exists because other sources of error may be obscuring this effect. It should also be pointed out that we do not have initial grain sizes for nearly half of the data points.

Recommendations by other investigators^{10,16,84} for an equiaxed grain growth temperature, irrespective of initial grain size, indicates that a value between 1400 and 1500°C is the most consistent.

Christensen⁸⁵ has presented the most reliable in-reactor measurements for a columnar grain growth temperature providing a mean temperature of $1648^{\circ}\text{C} \pm 62^{\circ}\text{C}$ (2σ) for 40 hours irradiation. These data were obtained from three capsules irradiated with three thermocouples each. The thermocouples were located at various radii on the fuel mid-plane, providing an accurate means of temperature measurement for grain growth.

For further insight into the selection of temperatures for grain growth, an analysis was performed to determine the temperature difference between the columnar and equiaxed boundaries. Equiaxed and columnar grain growth measurements from CEA-R-3358¹⁶ and CVNA-142⁸⁴ capsule experiments were used in the analysis. The mean of these data gave a temperature difference of 300°C with a 1σ uncertainty of 80°C .

Considering the above facts,

- the most consistent values quoted for equiaxed grain growth are between 1400 - 1500°C ,
- a best estimate for columnar grain growth is $\sim 1650^{\circ}\text{C}$, and

- the temperature difference between columnar and equiaxed grain growth temperatures is $\sim 300^\circ\text{C}$.

We have selected 1400°C and 1700°C as the temperature boundaries for equiaxed and columnar grain growth, respectively.

As will be discussed later in Correlating the Model to the Data, gas release data from experiments wherein thermocouples were used to measure fuel temperatures agree quite well with gas release data wherein grain growth boundaries were used to infer fuel temperatures. The good agreement indicates that the above estimates of grain growth temperatures are satisfactory.

As stated before, earlier attempts at calculating a radial temperature profile for gas release data were based on assumptions as to the gap conductance of the operating fuel rod. However, the uncertainties in estimating gap conductance can lead to errors as large as 500°C in centerline temperatures, while the errors associated with microstructural and thermocouple measurements can lead to errors (1σ) in centerline temperatures of $\sim 120^\circ\text{C}$ and $\sim 80^\circ\text{C}$ respectively (power and UO_2 thermal conductivity uncertainties are also included in these 1σ estimates). Because of the large error associated with assumed gap conductances, the latter two methods (microstructure and thermocouple measurements) were used to determine fuel temperatures rather than the less precise method of estimating gap conductance.

3.3 MODELS REVIEWED FOR HIGH TEMPERATURE GAS RELEASE

Existing models for gas release can be arranged into four categories:

1. those that correlate gas release against rod averaged conditions (either average heat rating or average temperature);
2. those that describe the movement of fission gas within the fuel solely on theoretical considerations;
3. those that correlate gas release against local operating conditions of the fuel;
4. and those that use an effective diffusion parameter, D' , to correlate gas release against a fuel temperature and time.

3.3.1 Volume Averaged Fuel Temperature

Models⁵ based on rod volume-averaged fuel temperatures are undesirable because actual gas release is dependent on local conditions and is a nonlinear function of temperature. Since temperatures vary both axially and radially within a cylindrical fuel column, gas release will also vary in the axial and radial directions.

If axial temperatures are held relatively constant (as was done with the selected data) and gas release is correlated against a local volume-averaged temperature in the radial direction, errors can still exist because the volume-average temperature is strongly weighted by the outer surface of the fuel, where temperatures are between 400 - 1200°C. It has been shown that gas release below 1200°C is negligible,^{8,25} while gas release from fuel in the columnar grain growth region (1700°C and above) has been shown^{9,10,22} to range from 70 - 95%. The central portion of the fuel, however, will have less influence on volume-average temperature. Gas release can be correlated against volume-average temperature with some degree of success because fuel surface temperatures for the majority of gas release data are in a narrow temperature range between 350 - 700°C, and for similar fuel capsule designs an increase in fuel surface temperature will correspond to a similar increase in the center temperature. It is still possible, however, that such a model can lead to significant errors in the prediction of gas release because the variable that is correlated against gas release, volume-average temperature, is strongly influenced by a temperature region which has negligible gas release. For example, it is possible to use a fuel capsule design which would provide a fuel surface temperature of 400°C and a centerline temperature of 2000°C, resulting in a volume-average temperature of 1113°C. Correspondingly, a capsule with the same volume-average temperature, but a lower heat rating, could have surface and centerline temperatures of 750 and 1515°C, respectively. The former capsule design will release a larger amount of gas because it has a substantial portion of fuel in the temperature region, 1700°C and above, while the latter design with a centerline of 1515°C has essentially no fuel in this high gas release zone.

An experiment performed by W. J. Zielenbach, et al.,²⁷ illustrates the high gas release rates exhibited in the temperature region of 1700°C and above. In this experiment several UO₂ capsules were irradiated with extremely high fuel surface temperatures (1200-1900°C). Capsules with fuel surface temperatures between 1700 - 1800°C and centerline temperatures between 1900 - 2100°C released 70 - 95% of their gas. The volume-average temperatures of these capsules were approximately 1900°C. Using the volume-average temperature model of Hoffman and Coplin,⁵ one would estimate that these capsules should release around 40% of their gas. This example points out the errors that can be encountered in applying the volume-average temperature model to a fuel design that is not typical of the data used to develop the model.

The models based on rod average heat rating⁶ have some obvious shortcomings in that fuel temperatures can vary significantly for different fuel rod designs at the same heat ratings. Data from different fuel rod designs correlated in this manner almost always have a large amount of variability. These models also have the same problems as volume-average temperature models, in that gas release is nonlinearly dependent on local conditions of the fuel, making a correlation based on averaged conditions subject to additional errors.

3.3.2 Theoretical Models

Using a theoretical model⁷ to describe the movement of fission gas within the fuel would be an ideal way to predict gas release; however, gas release on a theoretical basis has proven to be an extremely complex subject with many controlling parameters (both material and operating). This approach requires a rather large computer program just to simulate gas release and knowledge of a large number of physical parameters, which currently makes it impractical for a wide range of fuel designs. Also, it still remains to be proved that such a model can be used with a high degree of confidence and without any compensating assumptions to bring the model into agreement with the data.

3.3.3 Local Temperature Distribution

Empirical models¹ based on the local temperature distribution within the fuel are usually correlated against two different types of experiments: those experiments that measure local fission gas concentrations within the fuel by drilling small cores of fuel and measuring the retained gas, and those that measure the gas released from irradiated fuel capsules. The local temperature model can be semiquantitatively checked against the former type of experimental data; however, there is a large degree of variability within the retained gas data so that the accuracy of a model based entirely upon these data is questionable. A major source of variability in both types of data is in the estimate of the fuel temperatures and the variability of temperatures over the in-reactor irradiation history.

3.3.4 Effective Diffusion Coefficient Model

The use of an effective diffusion parameter, D' , to empirically fit a diffusion model against gas release was first used by Booth² and has subsequently been used by other investigators^{3,4} to describe both in-reactor and out-of-reactor gas release. Out-of-reactor data were not used in the present study; consequently, further discussions in this section are directed toward in-reactor data. Booth's derivation of this simple diffusion model from Fick's equations for volume diffusion depended on the assumption that an equivalent sphere can be used to approximate the boundary conditions for gas release. The approximate solution of Booth's model for small release fractions ($F < 0.2$) is:

$$F = 4 \sqrt{\frac{D't}{\pi}}$$

In this expression F is the fractional release of stable fission gas, t is the irradiation time and

$$D' = \frac{D}{a^2}$$

where a is the radius of the equivalent sphere and D is the diffusion coefficient used by classical diffusion theory. From diffusion theory

$$D = D_0 e^{-Q/RT}$$

where D_0 is a constant, Q is the activation energy, R is the gas constant and T is temperature. When D' is correlated against temperature the a^2 term is usually included in the D_0 term.

From this simple diffusion model it is predicted that gas release is a function of both temperature and time; however, as discussed in the section on Effects of Density and Burnup, the data that met our criteria show no burnup dependence (i.e., no time dependence). Disregarding the time dependence of a diffusion model still leaves the question as to what fuel temperature should be used to obtain the effective diffusion coefficient. The most logical approach would be a volume averaged temperature, but as discussed in the section on Volume Averaged Temperature errors can be introduced when fuel temperatures are volume averaged and correlated against gas release.

A local temperature model could be used wherein release fractions have been determined for specific temperature regions. From these fractions a D' could be determined for each temperature region. This method would be helpful in determining what diffusion mechanisms are controlling gas release and this should be pursued further to obtain a better mechanistic understanding of the process. It would be expected that different mechanisms will dominate within the various temperature regions.

Other approaches using the diffusion model are based on a separate determination of a^2 which is assumed to be a function of the surface-to-volume ratio which is in turn a function of fuel density. The gas release data used in this study did not show any dependence on fuel density.

Many of the models discussed above have been correlated against a substantial amount of data, but because a large amount of variability is associated with the data the uncertainties in the models are quite large. As stated earlier, the variability is often the result of poorly characterized data (e.g., with regard to temperatures, powers, O/M ratios, etc.).

3.4 SELECTION OF HIGH TEMPERATURE GAS RELEASE MODEL

The model chosen to describe the selected gas release data is based on local temperatures. We have selected the following regions within the fuel to describe high temperature gas release:

- columnar grain growth region, 1700°C and above
- equiaxed grain growth region, 1400 to 1700°C
- no microstructural change, 1200 to 1400°C

The form of our model is based on both experimental data and current theories for high temperature gas release. Gas release below 1200°C is described by the low temperature gas release model.

3.4.1 Columnar Grain Growth Region

Measurements of the fission gas concentrations within the columnar grain growth region indicate that between 70 to 95% of the gas produced in this region is released.^{9,22} Several investigators^{17,18} have proposed that the columnar grain growth region is a region of high mobility for pores containing gas, i.e., porosity from the fabrication process or that created by the accumulation of gas. These investigators suggest that the gas-filled pores become lenticular in shape and move up the temperature gradient toward the central void. Whatever the explanation for gas release in this region, it is apparent that the physical conditions within the region of columnar grain growth enhance gas release, as evidenced by the large fraction of gas released in the region.

3.4.2 Equiaxed Grain Growth Region

Measurements of the fission gas concentrations within the equiaxed grain growth region have indicated that between 10 to 40% of the gas produced in this region is released.^{9,22} Gas atoms and clusters of gas atoms within this region should be somewhat mobile because if the grain boundaries attain some degree of mobility as evidenced by grain growth there must be enough thermal energy present to allow some of the trapped fission gas to break away from the weaker trapping sites and find its way to an open pore.

3.4.3 Region of No Microstructural Change

Fission gas concentrations in the 1200 - 1400°C region indicate that less than 10% of the gas produced in this region is released.^{9,22} The experiments performed by Lewis²² indicate that for temperatures below 1200°C, nearly 100% of the gas is retained. Several other investigators^{8,25} have also concluded that the diffusion of fission gas below 1200°C is negligible. These conclusions are based on gas release data from fuel rods with centerline temperatures of less than 1200°C.

3.4.4 Description of Model

We have developed the following model for high temperature gas release:

$$F = AX_1 + BX_2 + CX_3$$

where

F = fraction of gas released

X_1 = fractional amount of fission gas produced in the temperature region 1200 to 1400°C

X_2 = fractional amount of fission gas produced in the temperature region 1400 to 1700°C (region of equiaxed grain growth)

X_3 = fractional amount of fission gas produced in the temperature region 1700°C and above (region of columnar grain growth)

A = fraction of gas released from region X_1

B = fraction of gas released from region X_2

C = fraction of gas released from region X_3

The fractional amount of gas produced in each of these regions (X_1 , X_2 and X_3) is estimated by taking the ratio of the cross-sectional area between the temperatures that bound the region to the total cross-sectional area of the pellet. The effects of flux depression are also included. The cross-sectional areas of each temperature region are obtained from the radial

temperature profiles that have been determined from the temperature data (thermocouple or microstructural) associated with each data point, as explained in the section on Data Reduction.

3.5 CORRELATING THE MODEL TO THE DATA

Using a multiple linear regression code, we fit the model to the reduced data (X_1 , X_2 and X_3) and obtained estimates of the coefficients A, B, and C associated with each temperature region. In the first attempt at a regression analysis, it was discovered that the X_1 and X_2 variables are linearly dependent on each other (i.e., $X_1 = GX_2$). Regressing X_1 against X_2 we find that $G = 0.727$. This dependency arises from the fact that if two temperature radii, such as the 1700°C and 1400°C boundaries used to obtain X_2 , are known within the radial cross-section of the fuel, then any other temperatures and their radii can be defined. A solution of the heat transfer equations will show that X_1 is linearly dependent on X_2 , but this is not covered here.

If data were available with centerline temperatures less than the upper boundary of X_2 (i.e., <1700°C), then X_1 would be independent of X_2 since only one temperature boundary defines X_2 and thus the coefficients A and B could be determined through regression analysis. Because all of the selected data contain centerline temperatures greater than 1700°C, we cannot separate these two coefficients due to the dependency between X_1 and X_2 . Consequently, the regression analysis was performed with the terms X_2 and X_3 to obtain the coefficients $B' = 0.177$ and $C = 0.807$ with a correlation coefficient of 0.980 and a residual standard deviation of 0.047 in fraction of gas released. The coefficient B' obtained in our regression analysis is a combination of the A and B coefficients of our model. Since X_1 can be related in terms of X_2 (over the range of our data) with the linear relationship $X_1 = GX_2$ (as discussed above), our model can be expressed in the following manner:

$$F = A (GX_2) + BX_2 + CX_3$$

The coefficient B' obtained from our regression analysis can be expressed by

$$B' = AG + B$$

and since $B' = 0.177$ and $G = 0.727$ a value for either A or B can be chosen on the basis of previous experimental evidence to get the other coefficient. As discussed earlier, experiments^{9,10,22,26} have been conducted in which small cores of fuel were ultrasonically drilled at various distances from the centerline of the pellet to determine the concentration of retained fission gas across the pellet radius. These experiments indicate that less than 10% of the gas produced in the 1200 - 1400°C range (X_1) and 10 - 40% in the region of equiaxed grain growth (X_2) is released. To be consistent with this evidence, we have selected a 5% release for region X_1 which yields 14.1% for the equiaxed region (i.e., $B = B' - A \cdot G = 0.177 - 0.05 (0.727) = 0.141$) to obtain our full model:

$$F = 0.050 X_1 + 0.141 X_2 + 0.807 X_3$$

Estimating the partitioning of the A and B coefficients in terms of B' does not compromise the accuracy of estimating gas release for fuel operating with centerline temperatures greater than 1700°C. Gas release for fuel with centerline temperatures between 1200°C and 1700°C is between 1% to 4%, as calculated from the high temperature model. An error in partitioning A and B can result in a maximum error of only 1% release for the above temperature range, even if there are gross errors in our partitioning of the A and B coefficients (as in the extreme case where $A = 0.0$ and $B = 0.177$). While the possible percentage error is great, it is doubtful that gas release measurements in these low release regions can be measured with greater accuracy. Also, in most fuel performance calculations it is not critical if the release rate is predicted to be 2% but is really only 1%; however, it does become critical if the release rates are predicted to be 30% but really are around 10%. Consequently, it is the higher gas release term ($0.807 X_3$) which is of greatest interest and has the largest influence on calculations for steady state operation. It should also be noted that the 80.7% release predicted in this analysis for the columnar grain growth region (X_3) agrees

quite well with the core drilling experiments which show that 70 - 95% of the gas in this region is released.

Predicted percent release as determined from the model is compared with the experimental data in Figure 1. If perfect agreement existed between the model and the data, all of the points would lie on the 45° sloped line which begins at the origin. The upper dashed line in this figure is the upper 95% confidence limit of our data which can be represented with the following relationship:

$$F = 0.050 X_1 + 0.141 X_2 + 0.807 X_3 + 1.68 (0.002112 + 0.0052 X_2^2 - 0.00269 X_2 X_3 + 0.00217 X_3^2)$$

where F , X_1 , X_2 and X_3 are the same variables used in the best estimate model.

The statistical significance of this upper limit is that you can be 95% confident that future gas release data, which meet the criteria we have used in selecting data, will lie below this line.

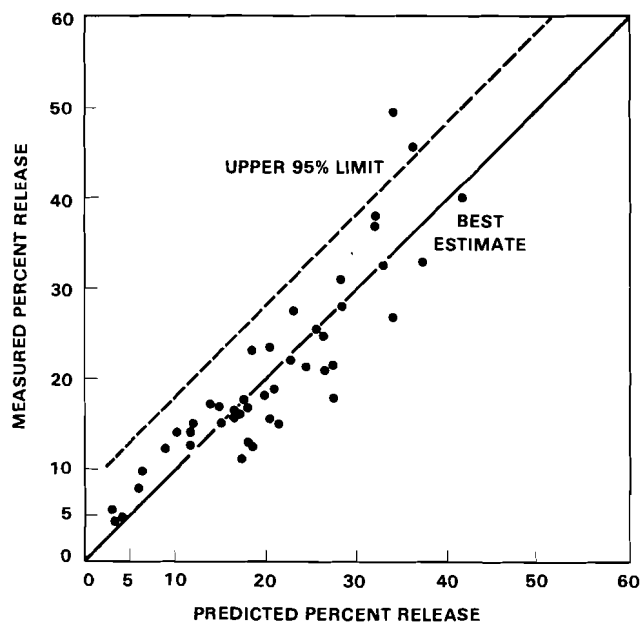


FIGURE 1. A Comparison of the High Temperature Release Model and the Data

As a check on the validity of our grain growth boundary temperatures, we compared the 41 data points based on grain boundaries to estimate fuel temperatures to the 4 data points that were obtained from thermocouple measurements. Good agreement between these two types of data is illustrated by placing a 1σ band around the data in Figure 1 and noting that three of the four thermocouple data lie within this band and the fourth within a 1.5σ band. This would indicate that our selection of grain growth temperatures is satisfactory.

A comparison of our model to models that have been proposed by other investigators^{1,5} is shown in Figures 2 and 3. Figure 2 shows the data and the relationship Hoffman and Coplin used in their volume-average temperature model. Also included is the proposed high temperature model expressed in terms of volume-average temperature, which was accomplished by selecting a typical commercial BWR fuel rod* and varying the power ratings while holding gap conductance constant at $1000 \text{ Btu/hr-ft}^2\text{-}^\circ\text{F}$ to insure the same fuel surface temperature as a function of power. The resulting temperature distributions were used to predict a value for gas release from our model and to calculate a volume-average fuel temperature to be used in plotting the curve for our high temperature model in Figure 2. This figure indicates that the scatter in the data used by Hoffman and Coplin is much larger than the scatter in the data used for the model developed here, as represented by the 95% confidence band. The 95% confidence band in Figure 2 bounds 95% of our data. This comparison provides additional support for the fact that the parameters we have controlled in the selection of the data do indeed lead to substantial amounts of variance between gas release data. The relationship developed here is also less conservative for volume-average fuel temperatures between 900 and 1525°C , which is the operating range of the peak power rods within most commercial LWR's. For example, at a volume-average temperature of 1200°C (fuel operating at $\sim 13 \text{ kw/ft}$) the Hoffman and Coplin model would predict a 24% increase while the best estimate model developed here would predict 13%.

*Changing the fuel rod design will shift the curve represented by the model. In most cases the shift is small for a particular reactor type because fuel rod designs are usually similar.

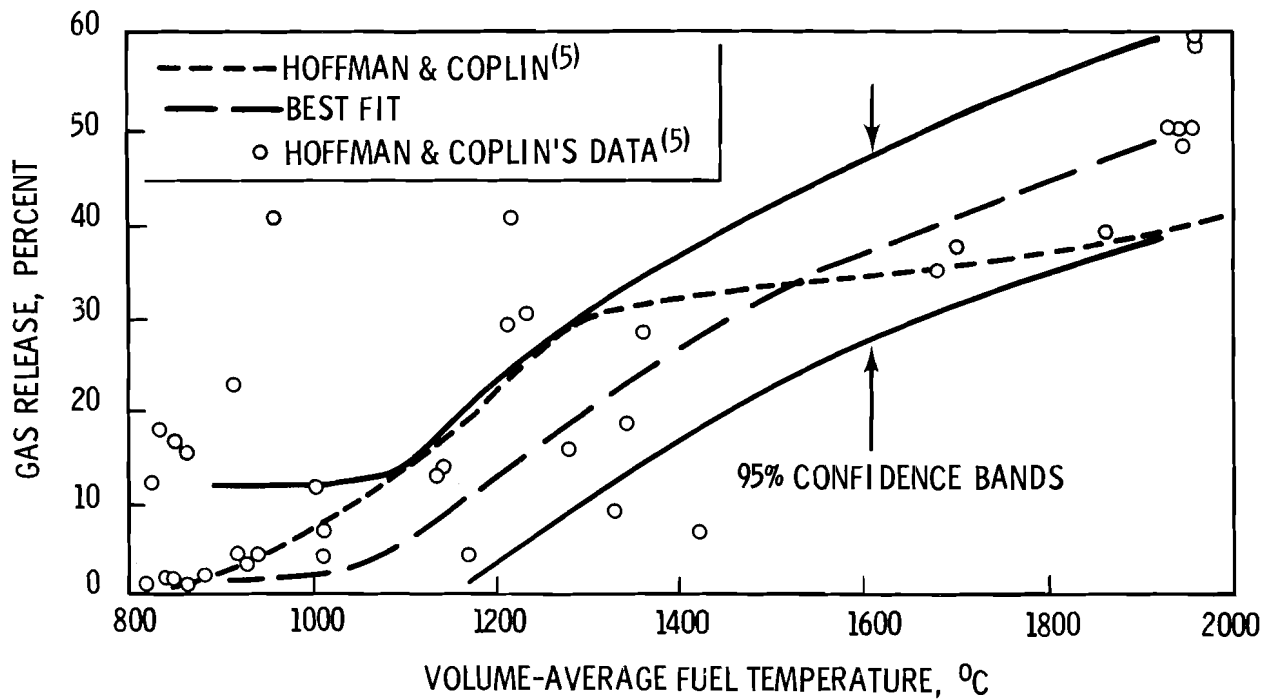


FIGURE 2. A Comparison of the High Temperature Release Model with Hoffman and Coplin's Volume-Average Temperature Model

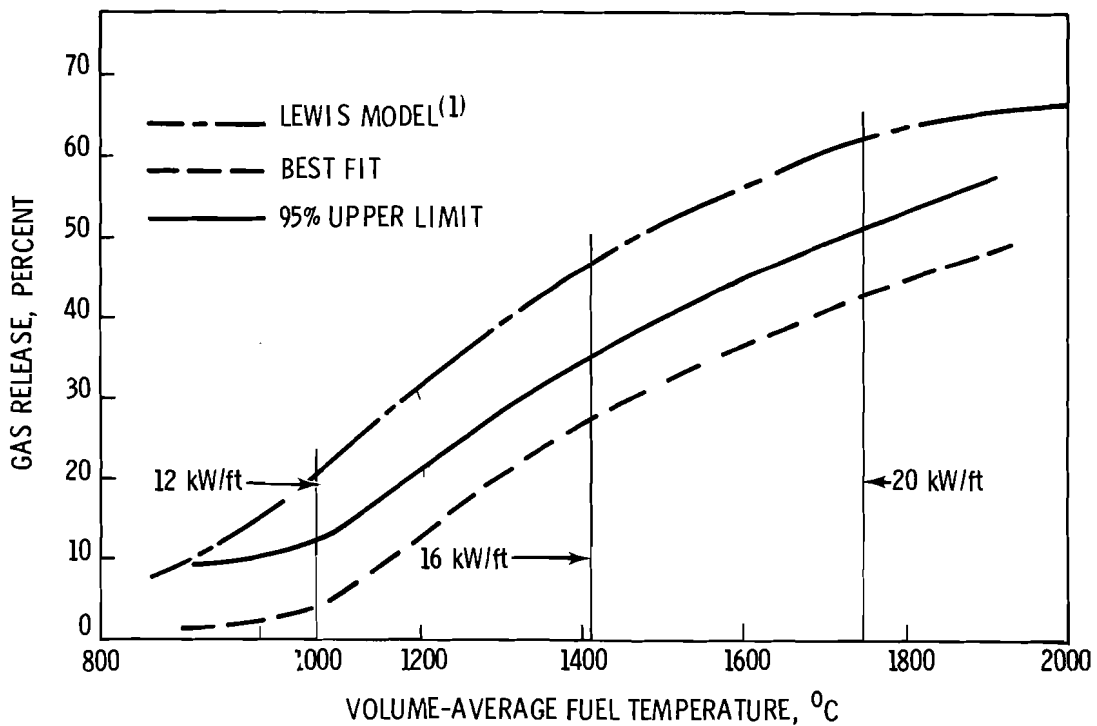


FIGURE 3. A Comparison of the High Temperature Release Model with Lewis' Model

Figure 3 shows a comparison of our model with the Lewis¹ model in terms of a volume-average temperature for a typical BWR fuel design. As seen here, the Lewis model is much more conservative than even the 95% upper limit of our relationship. This is not too surprising since Lewis intended the model to be conservative; however, it seems to be overly conservative in terms of the data and model reported here.

3.6 EFFECTS OF DENSITY AND BURNUP

There appears to be no general agreement on the effects of density and burnup on high temperature gas release for LWR UO₂ fuel. The range of the data with respect to the parameters of theoretical density and burnup is 91.3% TD to 98.0% TD and 400 MWD/MTM to 18,300 MWD/MTM. To determine if either of these two parameters have an effect on the data, a linear term was added for each of these parameters to the temperature dependent model already derived, as shown below:

$$F = AX_1 + BX_2 + CX_3 + DP$$

$$\text{and } F = AX_1 + BX_2 + CX_3 + KM$$

where A, B, C, X₁, X₂ and X₃ are the terms already described in the temperature dependent model and

D = coefficient describing the linear dependence
between density and gas release

P = percent of theoretical density

K = coefficient describing the linear dependence
between burnup and gas release

M = burnup

Fitting these two models against the data has shown that the linear coefficients for burnup and density, D and K, have a large amount of variance. Standard deviations associated with the linear coefficients, σ_D and σ_K , are approximately equal to the coefficients themselves. Using a t test to determine the probability that

$$D = 0 \text{ and } K = 0 \quad \left(\text{i.e., } t = \frac{D}{\sigma_D} \approx 1 \text{ and } t = \frac{K}{\sigma_D} \approx 1 \right)$$

shows that there is ~50% chance that $D = 0$ and $K = 0$ and thus indicates that neither burnup nor density has a significant influence on the data. If burnup or density effects were significant but nonlinear, the linear terms would still have been significant because they would have described some of the error structure in the data contributed by these two variables and resulted in lower values for σ_D and σ_K . As an additional check, the residual variance of each individual data point was plotted against both burnup and density and no structure was apparent within the data that might indicate a dependency on these two variables.

Although the data we have accumulated do not indicate any dependency between gas release and the two variables, burnup and density, this does not mean that such dependencies do not exist. There may be a small secondary effect within the range of our data; however, the error from other sources within the data obscures these effects. Also, it should be noted that the data covers the range of UO_2 densities 91.3 to 98.0% TD. Experimental evidence indicates that fuels with densities less than 90% TD release more gas than fuels with densities greater than 90% TD. In regard to a possible burnup dependency, it has been proposed by several investigators that the fission gas bubbles retained at the grain boundaries in fuel operating below 1700°C may become numerous enough to link up at high burnups and form a network by which gas can escape to an open pore and be released. Most of the data we collected from the literature have burnups between 4,000 MWD/MTM and 12,000 MWD/MTM, with a few data points going out to 18,000 MWD/MTM. We could not obtain data from well defined experiments on fuel designs typical of commercial thermal reactor fuel for burnups greater than 20,000 MWD/MTM. The need for such high burnup data is apparent since the high burnup rods in presently operating reactors may reach burnups of 40,000 - 50,000 MWD/MTM.

4.0 LOW TEMPERATURE GAS RELEASE MODEL

4.1 DEVELOPMENT OF THE MODEL

Low temperature gas release is dominated by a knock-out mechanism^{28,29} which is caused by a fission fragment passing through the fuel surface and ejecting a portion of the atoms near the surface. The material knocked out includes the matrix material and any trapped gas in that location. The amount of knock-out is a function of specimen surface area and irradiation dose.

The low temperature gas release model proposed by Bellamy and Rich⁸ was modified for this correlation. The Bellamy and Rich model was selected because it was the only one found in the literature that supplied and adequately described data applicable to LWR UO₂ fuel. The model expresses low temperature gas release in terms of the effective surface-to-volume ratio of the fuel, the fission rate, and the irradiation time in the following manner:

$$F = \frac{S}{V} \ell \left[\frac{3}{4} - \frac{3}{vft} \left\{ 1 - \exp \left(-\frac{1}{4} vft \right) \right\} \right] \quad (1)$$

where

F = fraction of gas release

S/V (%TD, BU) = effective surface-to-volume ratio of the fuel (a function of density and burnup), (cm⁻¹)

ℓ = recoil range of fission fragment (7 x 10⁻⁴ cm)

v = volume of fuel ejected from the fuel surface by "knock-out" (2 x 10⁻²¹ cm³)

f = fission rate, (fissions/cm³/sec)

t = irradiation time, (sec)

This relationship was derived by Bellamy and Rich from gas release data obtained from fuel rods over a wide range of burnups (7,000 - 43,000 MWD/MTM).

Fuel centerline temperatures were less than 1250°C for all the data, which is consistent with the high temperature model that assumes diffusional release is insignificant below 1200°C. Their data show a marked increase in gas release for burnups greater than 26,000 MWD/MTM. An experiment performed by Blieberg, et al.,³⁰ with flat plate UO₂ fuel elements also indicated that low temperature gas release increases by a substantial amount at high burnups. The increase is believed to arise partly from the interconnection of grain boundary gas bubbles and partly from the fracture under thermal stress of grain boundaries weakened by gas bubbles which increases the effective surface area of the fuel. This behavior is substantiated by the appearance of fuel structures at high burnups which show extensive intergranular porosity and grain boundary cracking. A plot of the effective surface-to-volume ratios, as determined from the data and equation of Bellamy and Rich for low temperature gas release, is shown in Figure 4. The data in Figure 4 are from fuel with an as-manufactured

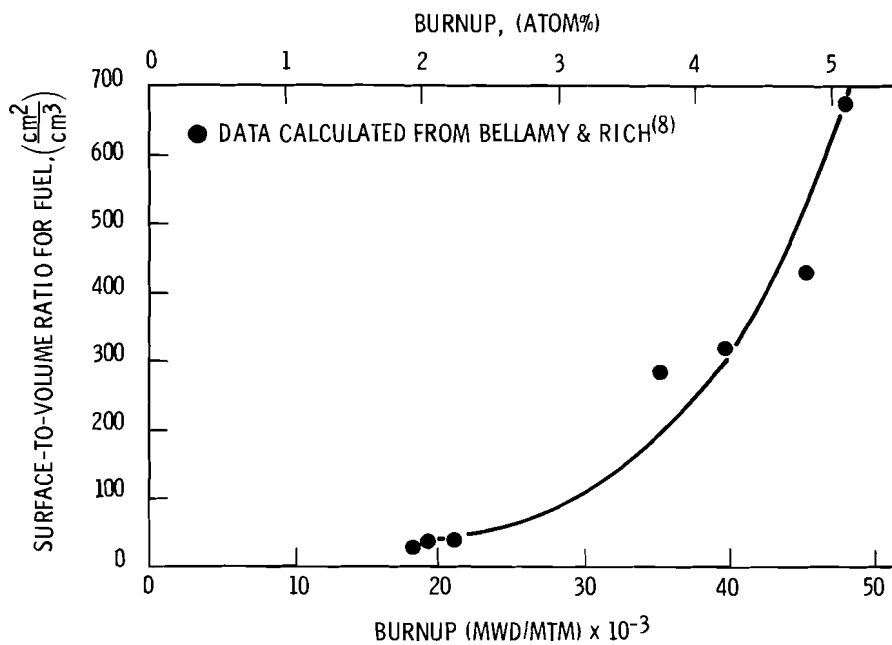


FIGURE 4. UO₂ Surface-To-Volume Ratios as a Function of Burnup

density of 98% TD. The increase in $\frac{S}{V}$ fits an exponential function fairly well for burnups of 17,000 MWD/MTM and greater by the following relationship:

$$\frac{S}{V} (\text{at burnup } X) = \frac{S}{V} (\text{initial}) 0.1938 \exp (+.9391X) \quad (2)$$

where

$$\frac{S}{V} (\text{initial}) = \text{initial surface-to-volume ratio (a function of the fuel density)}$$

$$X = \text{burnup in atom percent}$$

The functional relationship given in Figure 5 for the $\frac{S}{V}$ ratio in terms of the fuel as-manufactured theoretical density (i.e., $\frac{S}{V}$ [initial]) was taken from Lewis.³¹ By substituting the relationship for the surface-to-volume ratio as a function of burnup in Equation 2 into Equation 1, we can compare results from the low temperature release model with the data of Bellamy and Rich, as shown in Figure 6. The model predictions agree very well with this set of data. We have not attempted to correlate the low temperature release model to a large volume of data as was done with the high temperature release model because of the small effects of low temperature gas release on gap conductance calculations. This approach makes the accuracy of the model somewhat uncertain; however, in our opinion the model adequately describes low temperature gas release to within $\pm 1\%$ release.

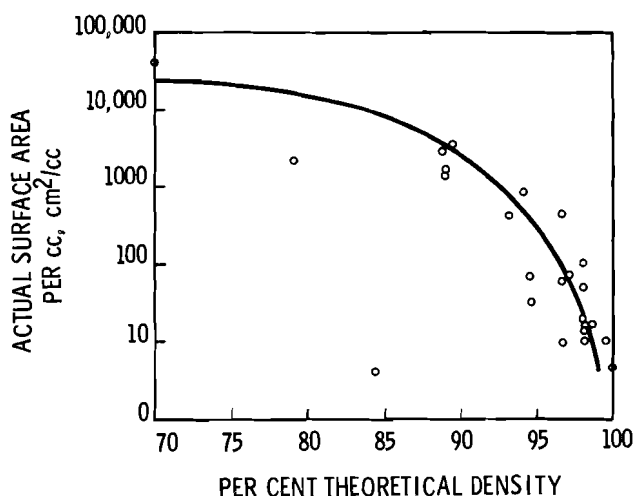


FIGURE 5. Measured Surface Area (BET) as a Function of Percent Theoretical Density for Sintered UO_2

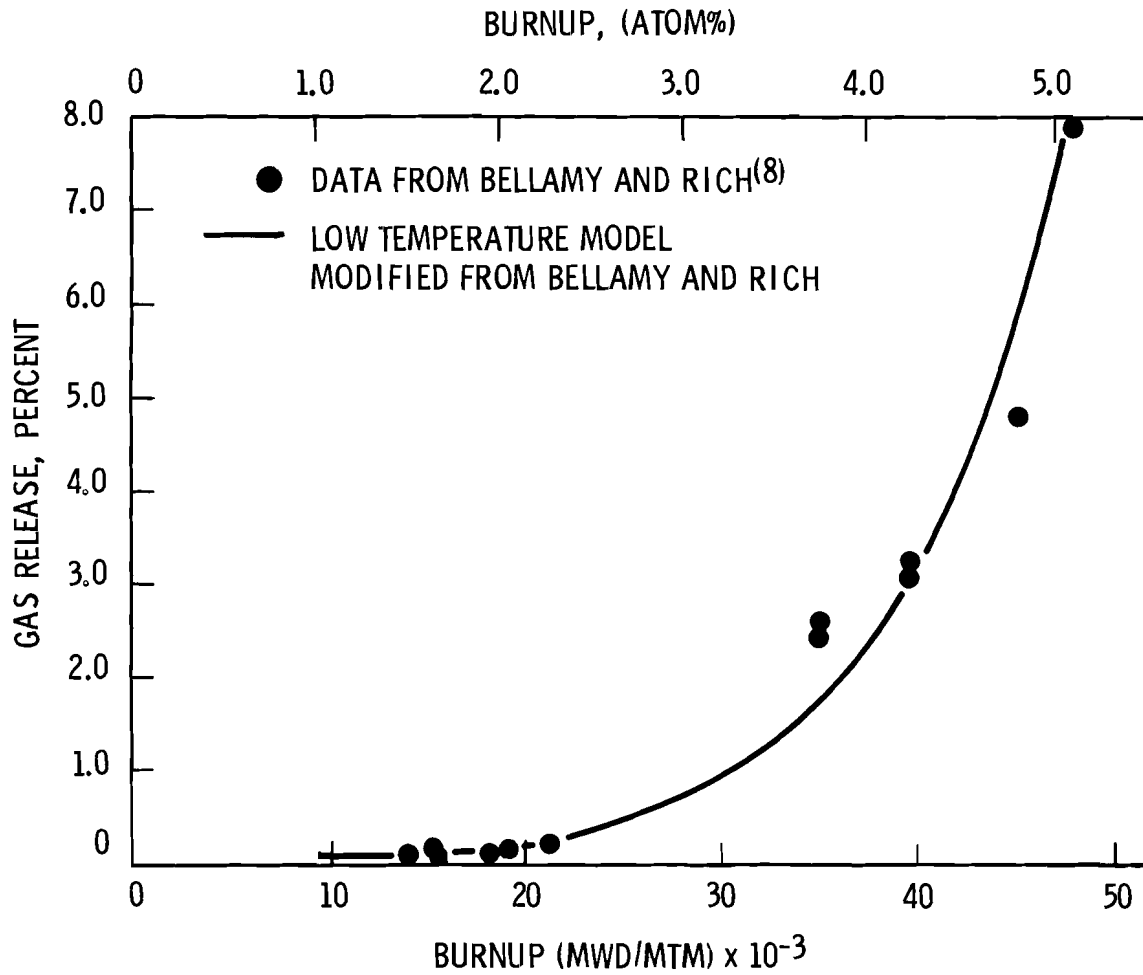


FIGURE 6. A Comparison of the Low Temperature Gas Release Model and the Data

5.0 LIMITATIONS OF THE GAS RELEASE MODELS

Neither model should be used beyond the range of data unless the extrapolated results can be checked against other sources of data. The models should not be used where a significant volume of the fuel is molten (>20%), because the molten fuel may release more than the maximum 80%. Although three data points used in the correlation have temperatures above the melting point of the fuel and they agree quite well with the model, these data points were from fuel rods with less than 20 volume-percent of the fuel molten. The high temperature model should also be restricted to the density and burnup range of our data, 91.3 - 98.0% TD and 400-18,300 MWD/MTM respectively. Although no density or burnup dependencies were found inside the range of our data there may be some strong dependencies outside this range, as was discussed in the section of Effects of Density and Burnup. The low temperature release model is limited to temperatures <1200°C and burnups <45,000 MWD/MTM and should be used in combination with the high temperature release.

Both models should be limited to steady state fuel operation until gas release data become available for significant power transients of a short time duration (e.g., accident transients). However, the models can be used for normal operating power changes, using the release algorithm developed by Notley^{8,8} which is based on experimental evidence from Souhier and Notley^{2,4} providing the new power level maintains an equilibrium value for several hours.

ACKNOWLEDGMENTS

The authors wish to acknowledge the support provided by the Core Performance Branch, Department of Regulatory and the reviews and suggestions provided by Dr. R. O. Meyer, G. Draney and R. Lobel.

We would also like to acknowledge the assistance of E. S. Gilbert in the statistical evaluation of the data and the comments from W. J. Bailey and F. E. Panisko.

REFERENCES

1. W. B. Lewis, "Engineering for the Fission Gas in UO_2 Fuel," Nucl. Appl., 2, (1966) p. 171.
2. A. H. Booth, A Method of Calculating Fission Gas Diffusion from UO_2 Fuel and its Application to the X-2-f Loop Test, AECL-496 (September 1957).
3. G. W. Parker, et al., "Prompt Release of Fission Products from Zircaloy-Clad UO_2 Fuels," in Nuclear Safety Program Annual Progress Report for Period Ending December 31, 1967, ORNL-4228, Oak Ridge National Laboratory (April, 1968).
4. D. L. Morrison, et al., An Evaluation of the Applicability of Existing Data to the Analytical Description of a Nuclear Reactor Accident, BMI-1779 (August 1966).
5. J. P. Hoffman and D. H. Coplin, The Release of Fission Gases from Uranium Dioxide Pellet Fuel Operated at High Temperatures, GEAP-4596 (September 1964).
6. V. F. Baston, et al., An Analytical Method for Calculating Steady-State Fission Gas Release--Fission Product Fuel Model (FPFM) Code, ANCR-1010, (September 1971).
7. H. R. Warner and F. A. Nichols, "A Statistical Fuel Swelling and Fission Gas Release Model," Nucl. Appl. and Tech. Vol. 9 (August 1970).
8. R. G. Bellamy and J. B. Rich, "Grain Boundary Gas Release and Swelling in High Burn-up Uranium Dioxide," J. Nucl. Mat. 33, 64-78, (1969).
9. P. Chenebault and R. Delmas, "Fission Gas Emission by Uranium Dioxide in Fuel Elements," ANL-TRANS-929, Conf.-720843-1 (August 1972).
10. J. P. Stora and P. Chenebault, Programme Cyrano-Mesure de l'intégrale de conductibilité thermique d' UO_2 fritté jusqu'a 2300°C - Evolution des gaz de fission a puissance constante, CEA-R-3618 (1968).
11. J. A. Ainscough, An Assessment of the IFA-116 and 117 Irradiations from Data Obtained from the In-Reactor Instrumentation, HPR-129, (April 1971).
12. E. De Meulemeester, et al., "Review of Work Carried out by BELGONCLEAIRE and CEA on the Improvement and Verification of the Computer Code with the Aid of In-Pile Experimental Results," British Nuclear Energy Society International Conference on Nuclear Fuel Performance (October 15-19, 1973).

13. M. J. F. Notley, R. Deshaies, et al., Measurements of the Fission Product Gas Pressures Developed in UO₂ Fuel Elements During Operation, AECL-2662 (1966).
14. M. J. F. Notley and J. R. MacEwan, The Effect of UO₂ Density of Fission Product Gas Release and Sheath Expansion, CRNL Report AECL-2230 (1965)
15. M. J. F. Notley, et al., Zircaloy Sheathed UO₂ Fuel Elements Irradiated at Values of ρ_{kd} Between 40 and 83 w/cm, AECL-1676, (December 1962).
16. Jean-Claude Janvier, et al., Irradiation of Uranium Dioxide in a Resistant Cladding Effects of Initial Diametral Gap on Overall Behavior CEA-R-3358, (October 1967).
17. F. A. Nichols, Behavior of Gaseous Fission Products in Oxide Fuel Elements, WAPD-TM-570 (October 1966).
18. R. M. Cornell and G. K. Williamson, J. Nucl. Mat. 17 (1965) 200 also A. J. Manley J. Nucl. Mat. 27 (1968) 244.
19. R. Souhler, "Fission-Gas Release from UO₂ During Irradiation Up to 2000°C," Nucl. Appl., 2, 138 (1966).
20. R. M. Carroll, et al., "Fission Density, Burnup, and Temperature Effects on Fission-Gas Release from UO₂," Nucl. Sci. & Eng. 38, 143-155, (1969).
21. J. A. L. Robertson, et al., Behaviors of Uranium Oxide as a Reactor Fuel." AECL-No. 603, September 1, 1958. Also GENEVA Conf. 1958, A/A/Conf./15/p. 193.
22. W. B. Lewis, et al., "Fission Gas Behavior in Uranium Dioxide Fuel," 3rd ICP UAE, p. 19 United Nations (1964).
23. R. Lindner and H. J. Matzke, "Diffusion of Xe-133 in Uranium Oxide of Different Oxygen Contents," Z. Naturforsch. 14 A, 582-584 (1959).
24. R. Souhler and M. J. F. Notley, "Effect of Power Changes on Fission Product Gas Release from UO₂ Fuel," Nucl. Appl. Vol. 5, p. 296.
25. W. W. Morgan, et al., A Preliminary Report on Radial Distribution of Fission-Product Xenon and Cerium in UO₂ Fuel Elements, AECL-1249 (April 1961).
26. P. Chenebault and R. Dumas, "In-Pile Mobility of Fission Gases in UO₂ Fuel Rods," Ceramic Nucl. Fuels (1969).
27. W. J. Zielenbach, et al., Irradiation Behavior of Oxide Fuels at High Temperatures, BMI-1925, (June 30, 1972).

43. D. L. Zimmerman, Irradiation and Post-Irradiation Examination of N. S. Savannah Test Fuel Element S1-A, GEAP-3342, January 28, 1960.
44. F. A. Brandt, et al., Irrad. Results, N.S. Savannah Core II prototype Fuel Assemb. (Assemb. SAV-II-2 & Sav-II-3), GEAP-3559, Nov. 7, 1960.
45. M. J. F. Notley, et al., "The Fission-Product Gas Pressures in UO₂ Fuel Elements During Irradiation," Trans. American Nuclear Society, 8, no. 2, 424. (Nov. 1965).
46. R. D. MacDonald & A. S. Bain, Irradiation of Zircaloy-2 Clad UO₂ to Study Sheath Deformation, CRNL Report AECL-1685 (1962).
47. J. A. L. Robertson, A. M. Ross, et al., "Temp. Distrib. in UO₂ Fuel Elements," J. Nucl. Mat. 7, 255 (1962).
48. A. M. Ross, "Irradiation Behavior of Fission Gas Bubbles and Sintering Pores in UO₂," J. Nucl. Mat. Vol. 30, No. 1 & 2, (1969).
49. R. S. Nelson, "The Stability of Gas Bubbles in an Irradiation Exper.," J. Nucl. Mat. 31, 153 (1969).
50. R. M. Cornell, et al., "The Role of Bubbles in Fission Gas Release from Uranium Dioxide," J. Nucl. Mat. 30, 170-178 (1969).
51. Brian R. T. Frost, "Theories of Swelling and Gas Retention in Ceramic Fuels," Nucl. Appl. & Tech. Vol. 9 (August 1970).
52. M. G. Balfour and J. F. Mellor, Post-Irradiation Examination of CVTR Fuel Assemblies, WCAP-3850-4, (August 1969).
53. W. A. Bezella, Analysis of the Fission Gases Released Within Spent Yankee Fuel Rods, WCAP-6087, (February 1968).
54. R. M. Carroll, "Fission Gas Effects in Reactor Fuels Part I. Basic Studies," Nucl. Safety. Vol. 12, No. 4, (July-August 1971).
55. R. M. Carroll and O. Sisman, "Behavior of Mixed Oxide (U, PU)O₂ Fuels as a Function of Temperature and Burnup," Nucl. Tech., Vol. 11, (August 1971).
56. Kazumi IWAMOTO and Jun OISHI, "Analysis of Fission Gas Escape from Reactor Fuel During Isothermal Irradiation," J. Nucl. Sci. & Tech., 5, 387, (August 1968).
57. Che-Yu Li, et al., "Some Consideration of the Fission Gas Bubbles in Mixed Oxide Fuels," Nucl. Appl. and Tech. 9 (August 1970).

28. B. G. Childs, "Fission Product Effects in Uranium Dioxide," J. Nucl. Matls. 9, No. 3 (1963) 217-244.
29. R. M. Carroll, "Fission-Gas Behavior in Fuel Materials," Nuclear Safety, Vol. 8 No. 4 (Summer 1967) 345-353.
30. M. L. Bleiberg, et al., Effects of High Burnup on Oxide Ceramic Fuels, WAPD-T-1455 (1962).
31. W. B. Lewis, Uranium Dioxide: Properties and Nuclear Applications, ed. J. Belle (U.S. Govt., Washington, 1961) Section 9.4.2.
32. G. W. Parker, et al., Out-of-Pile Studies of Fission-Product Release from Overheated Reactor Fuels at ORNL, 1955-1965, ORNL-3981, Oak Ridge National Laboratory (July 1967).
33. B. J. Buescher and R. O. Meyer, "Thermal-Gradient Migration of Helium Bubbles in Uranium Dioxide," J. Nucl. Mat. 48:143-156 (1973).
34. R. M. Carroll, et al., "Fission Gas Release During Fissioning in UO_2 ," Nucl. Appl., 2, 142 (1966) p. 145.
35. R. B. Perezze, "A Dynamic Method for In-Pile Fission-Gas Release Studies," *ibid.*, 151.
36. J. R. MacEwan and P. A. Morel, "Migration of Xenon Through a UO_2 Matrix Containing Trapping Sites," *ibid.*, 158.
37. M. J. F. Notley, et al., "The Effect of UO_2 Density on Fission Product Gas Release and Sheath Expansion," *ibid.*, 117.
38. A. D. Whapsham, "Electron Microscope Observation of Fission-Gas Bubble Distribution in UO_2 ," *ibid.*, 123.
39. C. N. Spalaris and F. H. Megerth, Residual and Fission Gas Release from UO_2 , GEAP-4314, July 1963.
40. R. D. Page, "Engineering and Performance of Canada's UO_2 Fuel Association for Heavy Water Power Reactors," IAEA Symposium on Heavy Water Power Reactors, Vienna (1967) also AECL-2949.
41. V. B. Lawson, et al., Thermal Experiment with a UO_2 Fuel Assembly, CRFD-915, March 1969, AECL, Chalk River, Canada.
42. M. B. Reynolds, "Experimental Measurements of Fission Gas Pressure in Operating Reactor Fuel Elements," Trans. American Nuclear Society, Vol. 5, No. 2, November 1962.

58. J. R. Findlay, et al., "The Emission of Fission Products from Uranium-Plutonium During Irradiation to High Burnup," J. Nucl. Mat. 35, 24-34, (1970).
59. R. L. Ritzman, et al., "Interpretations of Fission Gas Behavior in Refractory Fuels," Nucl. Appl. & Tech., Vol. 9, (August 1970).
60. M. Hurme, Observations of Fuel Pin Internal Pressure, HPR-110.
61. J. Weisman, et al., "Fission Gas Release from UO₂ Fuel Rods with Time Varying Power Histories," Trans. Am. Nucl. Soc., 12:900-01 (November 1969).
62. T. B. Burley and M. D. Freshley, "Internal Gas Pressure Behavior in Mixed-Oxide Fuel Rods During Irradiation," Nucl. Appl. & Tech. Vol. 9, (August 1970).
63. M. G. Balfour, CVTR Fission Gas Release, WCAP-3850-5.
64. W. A. Yuill, et al., Release of Noble Gases from UO₂ Fuel Rods, IN-1346, (November 1969).
65. D. G. Martin, "The Migration of Equilibrium Gas Bubbles in a Solid Subject to a Stress Gradient," J. Nucl. Mat. 33 (1969) 23-29.
66. Koreyuki Sheba, et al., "The Mechanisms of In-Pile Fission Gas Release from UO₂," J. Nucl. Mat. 48 (1973) 253-263.
67. J. D. Eichenberg, et al., Effects of Irradiation on Bulk UO₂, WAPD-183 (1957).
68. C. Lepscky, et al., "Experimental Investigation of In-Reactor Molten Fuel Performance," Nucl. Tech. Vol. 16 (November 1972).
69. W. E. Bailey, et al., "Effect of Temperature and Burnup on Fission Gas Release in Mixed Oxide Fuel," Ceramic Nuclear Fuels, Proceedings of the International Symposium, Nuclear Division of the American Ceramic Society, Inc., Special Publication No. 2 (May 1969).
70. R. D. MacDonald and A. S. Bain, "10,000 MWd/Tonne From UO₂ Clad in Thin Zircaloy," Trans. Am. Nucl. Soc., 7, 449-450 (November 1964).
71. Michael B. Weinstein, et al., "A Fission Gas Release Correlation for Uranium Nitride Fuel Pins," NASA-TN-7401.
72. Michael B. Weinstein, et al., "Fission-Gas-Release Rates from Irradiated Uranium Nitride Specimens," NASA TM X-2890.
73. R. M. Carroll, et al., Release of Fission Gas During Irradiation, ORNL-3050.

74. B. Rubin, Fission Gas Release PWR Core 1 Blanket Fuel Rods Upon Conclusion of Seed 1 Life, WAPD-TM-263 (1961).
75. J. A. L. Robertson, Irradiation Effects in Nuclear Fuels, p. 138, Gordon and Breach, Science Publishers Inc., 1969).
76. M. F. Lyons, et al., UO₂ Pellet Thermal Conductivity From Irradiation with Central Melting, GEAP-4624, 1964.
77. S. Y. Ogawa, E. A. Lees, and M. F. Lyons, Power Reactor High Performance UO₂ Program, GEAP-5591, 1968.
78. J. C. Maxwell, A Treatise on Electricity and Magnetism, Vol. I, 3rd Edition, Oxford University Press (1891), reprinted by Dover, New York (1954).
79. A. Eucken, "The Heat Conductivities of Ceramic Refractory, Calculations of Heat Conductivity from the Constituents," Forsch, Gebiete Ingenieurw, B3 Forschungsheft, No. 353, 1932.
80. C. R. Hann, C. E. Beyer and L. J. Parchen, GAPCON-THERMAL-1: A computer Program for Calculating the Gap Conductance in Oxide Fuel Pins, BNWL-1778 (September 1973).
81. J. A. L. Robertson, $\int kd\theta$ in Fuel Irradiations, CRFD-835 (1959).
82. D. R. Skeen and L. J. Page, Thermos/Battelle: The Battelle Version of the THERMOS Code, BNWL-516 (September 1967).
83. J. B. Ainscough, et al., "Isothermal Grain Growth Kinetics in Sintered UO₂ Pellets," J. Nucl. Mat., Vol. 49, 1973-74.
84. R. N. Duncan, Rabbit Capsule Irradiation of UO₂, CVNA-142, (June 1962).
85. J. A. Christensen, "Columnar Grain Growth in Oxide Fuels," Nucl. Trans.
86. H. Hausner, Grain Growth of UO₂ - Part I, GEAP-4315, EURAEC-871 (1963).
87. H. Hausner, Grain Growth of UO₂ - Part II, GEAP-4689, EURAEC-1836 (1965).
88. M. J. F. Notley, "A Computer Program to Predict the Performance of UO₂ Fuel Elements Irradiated at High Power Outputs to a Burnup of 10,000 MWd/MTM," Nucl. Appl. Vol. 9, p. 195 (Aug. 1970).

APPENDIX A

DESCRIPTION AND LISTING OF THE PROGRAM MAIN

APPENDIX A

DESCRIPTION AND LISTING OF THE PROGRAM MAIN

The computer code MAIN was developed to compute radial temperature profiles across cylindrical fuel specimens given a location and a temperature within the fuel. The fuel was divided into 50 annular rings and the temperature difference across each increment was calculated assuming that the thermal conductivity and volumetric heat generation are constant within each ring.* The heat balance on an annular ring can be written as:

$$(\text{heat in}) + (\text{heat generated}) = (\text{heat out})$$

$$\text{or } q_{r_i} + 2\pi \dot{q} \int r dr = 2\pi r \frac{dt}{dr}$$

where q_{r_i} = heat entering annular ring at r_i per unit length
(calculated from the total heat generation rate of the fuel, volume of fuel between center line and r_i , and the flux depression)

r_i = inside radius of annular ring

\dot{q} = heat generation for this particular annular ring
(calculated from the total heat generation rate of the fuel, volume of annular ring, and the flux depression).

k = thermal conductivity of the fuel

r = any radial position within the ring

By integrating this expression with respect to temperature and radius the following equation is found.

*This assumption is valid because the size of the rings are small enough that heat generation is relatively constant across them and because the ΔT across each ring is small and thus the variation of thermal conductivity is also small.

$$\int_{T_i}^{T_o} dT = \frac{1}{K} \left[\left(\frac{\dot{q} r_i^2}{2} - \frac{q_{r_i}}{2\pi} \right) \ln \frac{r_o}{r_i} - \frac{\dot{q}}{4} (r_o^2 - r_i^2) \right]$$

Using this equation and knowing the temperature at a node in the fuel ($r_{\text{known}}, T_{\text{known}}$) the temperature at the nearest outer boundary of an annular ring (r_o, T_o) can be calculated as follows: an average temperature of the ring is assumed; an appropriate thermal conductivity value is assigned; temperature drop across the increment and, therefore, average temperature is calculated; and the calculated average temperature is compared to the assumed value. If the assumed and calculated values do not agree, a new value is assumed and the process is repeated. When agreement is reached to within 1°F the process proceeds to the next annular ring and continues in this manner until the outside surface of the fuel is reached and the temperature profile from r_{known} and T_{known} to the surface of the fuel is known. A similar method is then used to obtain the temperature profile from r_{known} to the center line of the fuel.

The input data required to run the program is listed below:

<u>Variable</u>	<u>Variable Name</u>	<u>Location</u>	<u>Comments</u>
Linear Power (Kw/ft)	P	Cols. 1-10	---
Outer Pellet Radius (in.)	RFS	Cols. 11-20	---
Inner Pellet Radius (in.)	RVIOD	Cols. 21-30	---
Pellet Density	DEN	Cols. 31-40	Fractional density of the fuel pellet $\left(\frac{\% \text{ T.D.}}{100} \right)$
Enrichment	FR35	Cols. 41-50	Weight fraction of the U which is U-235

Temperature (°F)	TG	Cols. 51-60	Temperature within the fuel
Location of Temperature	FRACRG	Cols. 61-70	In terms of the fraction of pellet radius $\frac{R_{TG}}{RFS}$
No. of Data Points Input for Flux Depression	NFLUX	Cols. 71-75	If this is left blank the code will calculate its own flux depression values.

The data listed above are contained on the first card in columns 1 thru 75. If flux depressions are to be input (recommended for enrichments $\geq 4\%$) NFLUX additional cards are required with each card containing a diameter (inches) in columns 1-10 and the relative neutron flux at that diameter in columns 11-20. The cards must be arranged so that the diameters are either in ascending or descending order. As many cases can be input as desired with the flux depression cards (if desired) following each data card.

A listing of the code is given here along with a sample problem.

Listing of MAIN

PROGRAM MAIN
74/74 OPT=1
FTN 4.1+REL
06/20/74 17.45.03.

	PROGRAM MAIN(INPUT,OUTPUT,PUNCH,TAPE5=INPUT,TAPE6=OUTPUT)	MAIN	2
	DIMENSION RV(8,100),BB(8,100),Q(60),R(60),TT(60),TS(60),DUM(60),DD	MAIN	3
	XUM(60),QIN(60),TSR(60)	MAIN	4
5	TCOR(I,T)=((1.025/.95)*(D/(1.+(1.-D)*.5)))*((38.24/(402.4+T))+	MAIN	5
	X(5.1256E-13*((T+273.)**3)))	MAIN	6
	1 CONTINUE	MAIN	7
	READ(5,501) P,RFS,RVOID,DEN,FR35,TG,FRACRG,NFLUX	MAIN	8
	IF(P.LE.0) GO TO 999	MAIN	9
	PI=3.14159	MAIN	10
10	NF=11	MAIN	11
	FR38=(1-FR35)	MAIN	12
	JFS=2*RFS	MAIN	13
	DENSIT=10.97	MAIN	14
	IF (NFLX) 90,90,60	MAIN	15
15	90 CALL DEPRES(DENSIT,FR35,FR38,DFS,RV)	MAIN	16
	GO TO 80	MAIN	17
	60 READ(5,70) ((RV(I,J),I=1,2),J=1,NFLUX)	MAIN	18
	75 NF=NFLUX	MAIN	19
	80 CONTINUE	MAIN	20
20	C CALCULATE THE VOLUME HEAT GENERATION IN FUEL	MAIN	21
	QTOT=P*3413.	MAIN	22
	QFT3=QTOT/(PI*(RFS**2-RVOID**2))*144	MAIN	23
	C SET UP SYSTEM OF N NODES OF EQUAL THICKNESS,RADII IN FEET	MAIN	24
	N=50	MAIN	25
25	AA1=N	MAIN	26
	DR=(RFS-RVOID)/AA1/12.	MAIN	27
	RO=RFS/12.	MAIN	28
	DO 100 I=1,N	MAIN	29
	C R IS IN FEET	MAIN	30
30	R(I)=RO-DR*(I-1)	MAIN	31
	RRR=(2*R(I)-DR)*12.	MAIN	32
	RATIO=TRP(RRR,RV,2,NF)	MAIN	33
	RDR=R(I)-DR	MAIN	34
	Q(I)=PI*(R(I)**2-RDR**2)*RATIO*QFT3	MAIN	35
35	100 CONTINUE	MAIN	36
	C CORRECT FOR ACCUMULATION OF ERROR IN HEAT GENERATION	MAIN	37
	SUMQ=0.	MAIN	38
	DO 110 I=1,N	MAIN	39
40	110 SUMQ=SUMQ+Q(I)	MAIN	40
	CORR=QTOT/SUMQ	MAIN	41
	CORR1=CORR	MAIN	42
	DO 120 I=1,N	MAIN	43
	120 Q(I)=CORR*Q(I)	MAIN	44
	QIN(1)=QTOT-Q(1)	MAIN	45
45	DO 801 I=2,N	MAIN	46
	801 QIN(I)=QIN(I-1)-Q(I)	MAIN	47
	DO 130 I=1,N	MAIN	48
	130 R(I)=RFS/12.-DR*(I-1)	MAIN	49
	RGRAIN=FRACRG*RFS/12	MAIN	50
50	DO 140 I=1,N	MAIN	51
	IF (R(I).LE.RGRAIN) GO TO 150	MAIN	52
	140 CONTINUE	MAIN	53
	150 CONTINUE	MAIN	54
	RDG2=ABS(RGRAIN-R(I))	MAIN	55
55	IF (RDG2.LE.0.001) GO TO 155	MAIN	56
	RDG1=ABS(R(I-1)-RGRAIN)	MAIN	57
	IF (RDG1.LE.RDG2) GO TO 160	MAIN	58

Listing of MAIN

PROGRAM MAIN		7/74	OPT=1	FTN 4.1+PEL	06/20/74	17.45.03.
	155	CONTINUE			MAIN	59
		RGRAIN=R(I)			MAIN	60
60		M=I			MAIN	61
		GO TO 170			MAIN	62
	160	RGRAIN=R(I-1)			MAIN	63
		M=(I-1)			MAIN	64
	170	CONTINUE			MAIN	65
65	C	BEIN TEMPERATURE CALCULATIONS FROM A KNOWN TEMPERATURE			MAIN	66
	C	TO THE CENTER OF THE FUEL			MAIN	67
		DO 240 I=M,N			MAIN	68
		RZ=R(I)			MAIN	69
		RDR=R(I)-DR			MAIN	70
70		IF (I.GT.M) GO TO 180			MAIN	71
		TAV=TG			MAIN	72
		TZ=TG			MAIN	73
		TT(M)=TG			MAIN	74
		GO TO 190			MAIN	75
75		180 TAV=TT(I)			MAIN	76
		TZ=TT(I)			MAIN	77
	190	CONTINUE			MAIN	78
		TAVC=(TAV-32.)/1.8			MAIN	79
		TAVK=TAVC+273.			MAIN	80
80		C=57.8*TCOR(DEN,TAVC)			MAIN	81
		IF (RDR.LT.1.E-20) GO TO 200			MAIN	82
		TERM=(RDR**2/(RZ**2-RDR**2)-QIN(I)/Q(I))*ALOG(RZ/RDR)			MAIN	83
		GO TO 210			MAIN	84
	200	TERM=0.			MAIN	85
85		210 TT(I+1)=TZ+Q(I)/(2.*PI*C)*(1.5-TERM)			MAIN	86
		TAV1=(TZ+TT(I+1))/2			MAIN	87
		TTAV=TAV			MAIN	88
		DIFF=ABS(TAV-TAV1)			MAIN	89
		IF (DIFF-1.) 240,240,220			MAIN	90
90		220 TAV=TAV1			MAIN	91
		IME=IME+1			MAIN	92
		IF (IME-10) 190,230,230			MAIN	93
	230	WRITE (5,602) TTAV, TAV1			MAIN	94
	240	IME=0			MAIN	95
95		IF (RGRAIN.GE.R(1)) GO TO 295			MAIN	96
		QT=QIN(M-1)			MAIN	97
		DO 300 IK=2,M			MAIN	98
		I=M-IK+2			MAIN	99
		RZ=R(I)			MAIN	100
100		RRR=(2.*R(I)+DR)*12			MAIN	101
		RDR=R(I)+DR			MAIN	102
		RATIO=TERP(RRR,RV,2,NF)			MAIN	103
		Q(I)=PI*(RZ**2-RDR**2)*RATIO*QFT3			MAIN	104
	300	CONTINUE			MAIN	105
105	C	CORRECT FOR ACCJM			MAIN	106
		SUMQ=0.			MAIN	107
		DO 310 IK=2,M			MAIN	108
		I=M-IK+2			MAIN	109
	310	SUMQ=SUMQ-Q(I)			MAIN	110
110		QRR=(QTOT-QT)/SUMQ			MAIN	111
	C	BEIN TEMPERATURE CALCULATIONS FROM A KNOWN TEMPERATURE			MAIN	112
	C	TO THE OUTSIDE SURFACE OF THE FUEL			MAIN	113
		DO 320 IK=2,M			MAIN	114
		I=M-IK+2			MAIN	115

Listing of MAIN

PROGRAM MAIN	74/74 OPT=1	FTN 4.1*REL	06/20/74 17.45.03.
115	320 Q(I)=CORR*Q(I)	MAIN	116
	DO 290 IK=2,M	MAIN	117
	I=M-IK+2	MAIN	118
	RZ=R(I)	MAIN	119
	RORO=R(I)+DR	MAIN	120
120	IF (I.LT.M) GO TO 250	MAIN	121
	TAV=TG	MAIN	122
	TZ=TG	MAIN	123
	GO TO 250	MAIN	124
250	TAV=TT(I)	MAIN	125
125	TZ=TT(I)	MAIN	126
260	TAVC=(TAV-32.)/1.8	MAIN	127
	TAVK=TAVC+273	MAIN	128
	C=57.8*TCOP(DEN,TAVC)	MAIN	129
	TERM=(RZ**2/(RZ**2-RORO**2)-QIN(I-1)/Q(I))*ALOG(RZ/RORO)	MAIN	130
130	TT(I-1)=TZ+Q(I)/(2.*PI*C)*(1.5-TERM)	MAIN	131
	TAV1=(TZ+TT(I-1))/2	MAIN	132
	DIFF=ABS(TAV-TAV1)	MAIN	133
	IF (DIFF-1) 290,290,270	MAIN	134
270	TAV=TAV1	MAIN	135
135	IME=IME+1	MAIN	136
	IF(IME-10) 260,280,280	MAIN	137
280	WRITE(6,602) TTAV, TAV1	MAIN	138
290	IME=0	MAIN	139
C	VOLUME AVERAGE THE TEMPERATURE	MAIN	140
140	295 CONTINUE	MAIN	141
	TSR(IN+1)=RVOID	MAIN	142
	DO 400 I=1,N	MAIN	143
	3I=I	MAIN	144
400	TSR(I)=RFS-((RFS-RVOID)/AA1*(BI-1.0))	MAIN	145
145	VAFR=(TSR(1)**2-TSR(2)**2)*PI*((TT(1)+TT(2))*0.5)	MAIN	146
	DO 410 I=2,N	MAIN	147
	VAFR=VAFR+(TSR(I)**2-TSR(I+1)**2)*PI*((TT(I)+TT(I+1))*0.5)	MAIN	148
410	CONTINUE	MAIN	149
	VAVGT=VAFR/((RFS**2-RVOID**2)*PI)	MAIN	150
150	VAVGC=(VAVGT-32.)/1.8	MAIN	151
	DO 420 I=1,N	MAIN	152
	BB(1,I)=TT(I)	MAIN	153
	BB(2,I)=TSP(I)	MAIN	154
420	CONTINUE	MAIN	155
155	VJLIN=(RFS**2-RVOID**2)*PI	MAIN	156
	R1200=TERP(2192.,BB,2,N)	MAIN	157
	R1400=TERP(2552.,BB,2,N)	MAIN	158
	R1700=TERP(3092.,BB,2,N)	MAIN	159
	V1200=(R1200**2-R1400**2)*PI/VOLIN	MAIN	160
160	V1700=(R1700**2-RVOID**2)*PI/VOLIN	MAIN	161
	V1400=(R1400**2-R1700**2)*PI/VOLIN	MAIN	162
	RRR=2*R1200	MAIN	163
	RAT12=TERP(RRR,RV,2,NF)	MAIN	164
	RAT12=RAT12*CORR1	MAIN	165
165	RRR=2*R1400	MAIN	166
	RAT14=TERP(RRR,RV,2,NF)	MAIN	167
	RAT14=RAT14*CORR1	MAIN	168
	RRR=2*R1700	MAIN	169
	RAT17=TERP(RRR,RV,2,NF)	MAIN	170
170	RAT17=RAT17*CORR1	MAIN	171
	RRR=0.0	MAIN	172

Listing of MAIN

PROGRAM MAIN	7/74 DPT=1	FTN 4.1+REL	06/20/74 17.45.03.
	RATO=TERP(RRR,RV,2,NF)	MAIN	173
	RATO=RATO*CORR1	MAIN	174
175	VCD12=V1200*(RAT12+RAT14)/2	MAIN	175
	VCD14=V1400*(RAT14+RAT17)/2	MAIN	176
	VCD17=V1700*(RAT17+RAT0)/2	MAIN	177
	FRACGR=0.21285*VCD14+0.79889*VCD17	MAIN	178
	TFS=TT(1)	MAIN	179
	TCL=TT(51)	MAIN	180
180	DO 500 I=1,N	MAIN	181
	TS(I)=R(I)*12	MAIN	182
	DUM(I)=(TT(I)-32.)/1.8	MAIN	183
	DOUM(I)=(TS(I)*2.54)	MAIN	184
185	500 CONTINUE	MAIN	185
	WRITE(6,700)	MAIN	186
	WRITE(6,605) P,RFS,RVOID,DEN,FR35,TG,FRACGR	MAIN	187
	WRITE(6,705)	MAIN	188
	WRITE(6,606)	MAIN	189
190	WRITE(6,607) (RV(1,J),RV(2,J),J=1,NF)	MAIN	190
	WRITE(6,710)	MAIN	191
	WRITE(6,715) VAVGT,VAVGTC,VCD12,VCD14,VCD17	MAIN	192
	WRITE(6,603) (TS(I),TT(I),DOUM(I),DUM(I),I=1,N)	MAIN	193
	GO TO 1	MAIN	194
	999 STOP	MAIN	195
195	70 FORMAT(2F10.0)	MAIN	196
	601 FFORMAT(7F10.0,I5)	MAIN	197
	602 FORMAT(1H0,"NO CONVERGENCE TEMP=",F7.2," CALCULATED TEMP.",F7.2	MAIN	198
	X,/))	MAIN	199
	603 FORMAT(1H0,	MAIN	200
200	X24X,"RADIUS",10X,"TEMPERATURE",15X,"RADIUS",12X,"TEMPERATURE",/,24	MAIN	201
	XX,"(INCHES)",11X,"(DEG F)",18X,"(CM)",15X,"(DEG C)",/, (24X,F6.4,9X	MAIN	202
	X,F10.2,17X,F6.4,13X,F10.2,))	MAIN	203
	605 FORMAT(/,	MAIN	204
205	X40X,"HEAT RATING",4X,F6.2,2X,"KW/FT",/	MAIN	205
	X40X,"FUEL RADIUS",4X,F8.5,2X,"INCHES",/	MAIN	206
	X40X,"CENTER VOID RADIUS",4X,F8.5,2X,"INCHES",/	MAIN	207
	X40X,"FUEL DENSITY",4X,F8.5,2X,/	MAIN	208
	X40X,"WEIGHT FRACTION U235",4X,F8.5,2X,/	MAIN	209
210	X40X,"COLUMAR GRAIN GROWTH TEMP.",4X,F8.0,2X,"DEG F",/	MAIN	210
	X40X,"FRACTION OF RADIUS FOR CGG",4X,F8.5,2X,/))	MAIN	211
	606 FORMAT(/,40X,"DIAMETER (IN)",12X,"FLUX RATIO",/)	MAIN	212
	607 FORMAT(43X,F6.4,19X,F6.4)	MAIN	213
	700 FORMAT(1H1,/,/,45X,"***** INITIAL INPUT DATA *****",)	MAIN	214
	705 FFORMAT(37X,"**** INPUT OR CALCULATED FLUX DEPRESSIONS ****",)	MAIN	215
215	710 FFORMAT(/,40X,"***** CALCULATED VALUES *****",/)	MAIN	216
	715 FFORMAT(24X,"AVERAGE VOLUMETRIC FUEL TEMPERATURE",2X,F8.2,2X,"DEG.F	MAIN	217
	X(",F8.2,1X,"DEG.C)",/)	MAIN	218
	X24X,"FRACTION OF GAS PRODUCED IN THE 1200-1400 DEG. C TEMPERATURE	MAIN	219
220	XREGION",2X,F8.6,/,	MAIN	220
	X24X,"FRACTION OF GAS PRODUCED IN THE 1400-1700 DEG. C TEMPERATURE	MAIN	221
	XREGION",2X,F8.6,/,	MAIN	222
	X24X,"FRACTION OF GAS PRODUCED IN THE 1700-**** DEG. C TEMPERATURE	MAIN	223
	XREGION",2X,F8.6,/,)	MAIN	224
	END	MAIN	225

Listing of MAIN

FUNCTION	TERP	74/74	OPT=1	FTN 4.1+REL	06/20/74	17.43.11.
			FUNCTION TERP(TT, TABLE, L, N)		TERP	2
			L = THE INDEX TO THE TABLE		TERP	3
			DIMENSION TABLE(8,100)		TERP	4
			I=1		TERP	5
5			IF (TABLE(I,1).GT.TABLE(I,N)) GO TO 110		TERP	6
			IF (TT.LE.TABLE(I,1)) GO TO 104		TERP	7
			IF (TT.GE.TABLE(I,N)) GO TO 106		TERP	8
			DO 100 J=1,N		TERP	9
			IF (TT-TABLE(1,J)) 101,102,100		TERP	10
10		100	CONTINUE		TERP	11
		104	TERP = TABLE(L,1)		TERP	12
			RETURN		TERP	13
		106	TERP = TABLE(L,N)		TERP	14
			RETURN		TERP	15
15		102	TERP = TABLE(L, J)		TERP	16
			RETURN		TERP	17
		101	TERP=TABLE(L, J-1)+(TABLE(L, J)-TABLE(L, J-1))*(TT-TABLE(I, J-1)) /		TERP	18
			X(TABLE(I, J)-TABLE(I, J-1))		TERP	19
			RETURN		TERP	20
20		110	IF (TT.GE.TABLE(I,1)) GO TO 104		TERP	21
			IF (TT.LE.TABLE(I,N)) GO TO 106		TERP	22
			DO 120 J=1,N		TERP	23
			IF (TT-TABLE(1,J)) 120,102,101		TERP	24
25		120	CONTINUE		TERP	25
			END		TERP	26

Listing of MAIN

SUBROUTINE	DEPRES	74/74	OPT=1	FTN 4.1+REL	06/20/74	17.45.14.
					DEPRES	2
					DEPRES	3
					DEPRES	4
					DEPRES	5
5					DEPRES	6
					DEPRES	7
					DEPRES	8
					DEPRES	9
					DEPRES	10
10					DEPRES	11
					DEPRES	12
					DEPRES	13
					DEPRES	14
					DEPRES	15
15					DEPRES	16
					DEPRES	17
					DEPRES	18
20					DEPRES	19
					DEPRES	20
20					DEPRES	21

Output From Sample Problem

***** INITIAL INPUT DATA *****

```

HEAT RATING                17.80  KW/FT
FUEL RADIIJS              .38190  INCHES
CENTER VOID RADIUS        0.00000  INCHES
FUEL DENSITY              .95700
WEIGHT FRACTION U235      .02400
COLUMAR GRAIN GROWTH TEMP. 3092.  DEG F
FRACTION OF RADIUS FOR CGG .26900
    
```

**** INPUT OR CALCULATED FLUX DEPRESSIONS ****

DIAMETER (IN)	FLUX RATIO
0.0000	1.0000
.0764	1.0038
.1528	1.0152
.2291	1.0343
.3055	1.0613
.3819	1.0966
.4583	1.1406
.5347	1.1937
.6110	1.2566
.6874	1.3300
.7638	1.4147

***** CALCULATED VALUES *****

```

AVERAGE VOLUMETRIC FUEL TEMPERATURE  1895.97  DEG.F ( 1035.54  DEG.C)
FRACTION OF GAS PRODUCED IN THE 1200-1400 DEG. C TEMPERATURE REGION  .114368
FRACTION OF GAS PRODUCED IN THE 1400-1700 DEG. C TEMPERATURE REGION  .156872
FRACTION OF GAS PRODUCED IN THE 1700-**** DEG. C TEMPERATURE REGION  .056997
    
```

RADIUS (INCHES)	TEMPERATURE (DEG F)	RADIUS (CM)	TEMPERATURE (DEG C)
.3819	740.28	.9700	393.49
.3743	809.56	.9506	431.98
.3666	880.11	.9312	471.17
.3590	951.82	.9118	511.01
.3513	1024.59	.8924	551.44
.3437	1098.29	.8730	592.38
.3361	1172.79	.8536	633.77
.3284	1247.96	.8342	675.53
.3208	1323.65	.8148	717.58
.3132	1399.72	.7954	759.84
.3055	1476.00	.7760	802.22
.2979	1552.35	.7566	844.64
.2902	1628.61	.7372	887.00
.2826	1704.59	.7178	929.22
.2750	1780.15	.6984	971.19
.2673	1855.11	.6790	1012.84
.2597	1929.30	.6596	1054.06
.2521	2002.58	.6402	1094.77
.2444	2074.78	.6208	1134.88
.2368	2145.75	.6014	1174.30
.2291	2215.34	.5820	1212.97

.2215	2283.42	.5626	1250.79
.2139	2349.86	.5432	1287.70
.2062	2414.54	.5238	1323.63
.1986	2477.35	.5044	1358.53
.1910	2538.19	.4850	1392.33
.1833	2596.98	.4656	1424.99
.1757	2653.63	.4462	1456.46
.1680	2708.08	.4268	1486.71
.1504	2760.27	.4074	1515.70
.1528	2810.14	.3880	1543.41
.1451	2857.67	.3686	1569.82
.1375	2902.81	.3492	1594.89
.1298	2945.53	.3298	1618.63
.1222	2985.83	.3104	1641.01
.1146	3023.67	.2910	1662.04
.1069	3059.07	.2716	1681.70
.0993	3092.00	.2522	1700.00
.0917	3122.47	.2328	1716.93
.0840	3150.47	.2134	1732.48
.0764	3176.01	.1940	1746.67
.0687	3199.10	.1746	1759.50
.0611	3219.74	.1552	1770.97
.0535	3237.93	.1358	1781.07
.0458	3253.67	.1164	1789.82
.0382	3266.99	.0970	1797.22
.0306	3277.87	.0776	1803.26
.0229	3286.34	.0582	1807.97
.0153	3292.38	.0388	1811.32
.0076	3296.00	.0194	1813.33

***** INITIAL INPUT DATA *****

HEAT RATING	17.10	KW/FT
FUEL RADIJS	.32126	INCHES
CENTER VOID RADIUS	0.00000	INCHES
FUEL DENSITY	.97900	
WEIGHT FRACTION U235	.04500	
COLUMAR GRAIN GROWTH TEMP.	3092.	DEG F
FRACTION OF RADIUS FOR CGG	.31000	

**** INPUT OR CALCULATED FLUX DEPRESSIONS ****

DIAMETER (IN)	FLUX RATIO
0.0000	1.0000
.1600	1.0163
.2410	1.0442
.3210	1.0834
.4020	1.1356
.4820	1.2004
.5620	1.2793
.6425	1.3740

***** CALCULATED VALUES *****

AVERAGE VOLUMETRIC FUEL TEMPERATURE	2007.26	DEG.F (1097.37 DEG.C)
FRACTION OF GAS PRODUCED IN THE 1200-1400 DEG. C TEMPERATURE REGION	.123347	
FRACTION OF GAS PRODUCED IN THE 1400-1700 DEG. C TEMPERATURE REGION	.169069	
FRACTION OF GAS PRODUCED IN THE 1700-**** DEG. C TEMPERATURE REGION	.077292	

RADIUS (INCHES)	TEMPERATURE (DEG F)	RADIUS (CM)	TEMPERATURE (DEG C)
.3213	872.43	.8160	466.90
.3148	942.48	.7997	505.82
.3084	1013.59	.7834	545.33
.3020	1085.65	.7670	585.36
.2956	1158.53	.7507	625.85
.2891	1232.12	.7344	666.74
.2827	1306.29	.7181	707.94
.2763	1380.91	.7018	749.39
.2599	1455.82	.6854	791.01
.2634	1530.89	.6691	832.72
.2570	1605.96	.6528	874.42
.2506	1680.89	.6365	916.05
.2442	1755.51	.6202	957.50
.2377	1829.67	.6038	998.71
.2313	1903.23	.5875	1039.57
.2249	1976.02	.5712	1080.01
.2185	2047.90	.5549	1119.94
.2120	2118.71	.5386	1159.28
.2056	2188.33	.5222	1197.96
.1992	2256.61	.5059	1235.90
.1928	2323.44	.4896	1273.02
.1863	2388.69	.4733	1309.27
.1799	2452.25	.4570	1344.58
.1735	2514.02	.4406	1378.90

.1671	2573.92	.4243	1412.18
.1606	2631.86	.4080	1444.36
.1542	2687.77	.3917	1475.43
.1478	2741.58	.3754	1505.32
.1414	2793.26	.3590	1534.83
.1349	2842.74	.3427	1561.52
.1285	2889.99	.3264	1587.77
.1221	2934.98	.3101	1612.77
.1157	2977.69	.2938	1636.50
.1092	3018.11	.2774	1658.95
.1028	3056.22	.2611	1680.12
.0964	3092.00	.2448	1700.00
.0900	3125.46	.2285	1718.59
.0835	3156.60	.2122	1735.89
.0771	3185.42	.1958	1751.90
.0707	3211.92	.1795	1766.62
.0643	3236.10	.1632	1780.06
.0578	3257.97	.1469	1792.20
.0514	3277.52	.1306	1803.06
.0450	3294.75	.1142	1812.64
.0386	3309.67	.0979	1820.93
.0321	3322.28	.0816	1827.93
.0257	3332.59	.0653	1833.66
.0193	3340.60	.0490	1838.11
.0129	3346.32	.0326	1841.29
.0064	3349.75	.0163	1843.19

APPENDIX B

Reduced Fuel Temperatures

TABLE B-1. Reduced Fuel Temperature

REFERENCE	SPECIMEN NUMBER	HEAT RATING (kw/ft)	SURFACE TEMPERATURE (°C)	CENTERLINE TEMPERATURE (°C)	GAS RELEASE (PERCENT)
CYRANO EXP.	CYRANO-II	13.9	752/758	1990/2069*	15.0
	CYRANO	11.5	819/843	1890/1969*	13.0
HPR-129	116-5	22.8	360/341	2070/2374*	27.5
	117-1	21.0	530/512	2060/2329*	25.4
BELGONUCLEAIRE AND CEA	EPL-4	12.3	617/ - †	1743/ - †	9.9
	EPL-5	13.5	513/ - †	1693/ - †	4.4
	EPL-6	15.1	670/688†	2133/2160†	21.3
	EPL-9	14.9	600/618	2000/2030	23.2
	EPL-10	14.9	600/656	2000/2089	18.3
	EPL-12	13.3	691/674	1971/1945	17.8
AECL-2662	LFL	18.0	351/ -	1678/ -	5.7
	LFF	17.8	473/ -	1974/ -	17.3
	LFB	17.3	540/551	2108/2128	23.4
	LFS	24.5	450/509	2500/2596	37.9
	LFW	25.0	343/403	2343/2459	24.8
	LFT	24.1	490/500	2679/2694	49.6
	LFX	24.9	453/467	2614/2638	36.8
	LFM	22.7	357/431	2156/2305	15.5
	LFH	22.1	495/502	2434/2447	31.1
LFD	22.1	546/606	2586/2673	45.8	
AECL-2230 (TEST X-501)	CBN	17.1	443/467	1797/1843	12.3
	CBO	17.3	435/490	1802/1843	14.9
	CB	16.8	432/483	1762/1862	14.1
	CBR	17.4	459/534	1880/2019	15.7
	CBT	16.6	446/545	1795/1981	15.3
	CBV	17.5	425/515	1854/2027	16.5
	CBY	16.55	471/565	1871/2043	16.8
	CBX	17.1	471/579	1923/2117	18.8
AECL-1676 (TEST X-211)	DFE	35.8	- /399	- /3248	40.1
	DFH	29.5	- /385	- /2799	32.6
	DFD	29.05	- /476	- /2903	33.0
	DFB	24.0	- /458	- /2469	17.9
	DFA	17.7	391/ -	1734/ -	4.95
CEA-R-3358	4110-AE1	18.1	612/ -	2296/ -	21.6
	-AE2	17.6	570/ -	2175/ -	22.1
	-BE1	15.1	548/ -	1876/ -	13.9
	-BE2	17.8	485/ -	2047/ -	15.9
	4112-AE1	19.5	440/399	2167/2085	12.6
	-AE2	17.7	504/462	2097/2019	11.2
	-BE1	15.4	425/ -	1699/ -	7.9
	-BE2	16.6	498/427	1971/1832	12.6
	4113-AE1	17.1	731/725	2419/2426	26.7
	-AE2	15.6	756/701	2278/2199	28.0
	-BE1	16.0	532/544	1942/1988	17.0
	-BE2	15.9	718/670	2239/2169	21.0

* TEMPERATURE MEASUREMENT BY A THERMOCOUPLE AT FUEL CENTERLINE/CORRECTED CENTERLINE TEMPERATURES FOR THAT PORTION OF THE FUEL WITHOUT AN ANNULAR HOLE AND THERMOCOUPLE

† TEMPERATURE DETERMINED FROM EQUIAXED BOUNDARY/TEMPERATURE DETERMINED FROM COLUMNAR BOUNDARY

NOTE: SEE TABLE 1 IN REPORT FOR MORE INFORMATION

DISTRIBUTION

No. of
Copies
Offsite

1 AEC Chicago Patent Attorney
A. A. Churm

199 AEC Technical Information Center

1 AEC Division of Reactor Safety Research, Washington, D.C.
Director

1 AEC Technical Review, Licensing, Washington, D.C.
Deputy Director

1 AEC Reactor Projects, Licensing, Washington, D.C.
Deputy Director

1 AEC Fuels and Materials, Licensing, Washington, D.C.
Deputy Director

1 AEC Reactor Safety, Licensing, Washington, D.C.
Assistant Director

1 AEC Containment Safety, Licensing, Washington, D.C.
Assistant Director

1 AEC Plans & Programs, Reactor Standards, Washington, D.C.
Assistant Director

6 AEC Reactor Systems Branch, Licensing, Washington, D.C.
Chief

25 AEC Core Performance Branch, Licensing, Washington, D.C.
Chief

No. of
Copies
Offsite

- 1 AEC Fuels and Materials Branch, Reactor Research and Development
Washington, D.C.
Chief
- 1 AEC Fuels and Materials Branch, Regulatory Standards Branch
Washington, D.C.
Chief
- 2 AEC Fuel Behavior Branch, Regulatory Standards Branch
Washington, D.C.
Chief

No. of
Copies
Onsite

- 1 AEC Richland Operations Office
B. J. Melton
- 38 Battelle-Northwest
W. J. Bailey
C. E. Beyer (10)
J. W. Finnigan
M. D. Freshley
S. Goldsmith
C. R. Hann (10)
R. R. Lewis
R. K. Marshall
C. L. Mohr
P. J. Pankaskie
L. J. Parchen
D. D. Lanning
F. E. Panisko
R. P. Marshall
J. A. Christensen
D. W. Brite
Technical Information Files (3)
Technical Publications